Journal for ImmunoTherapy of Cancer

Clinical and molecular characteristics associated with response to therapeutic PD-1/PD-L1 inhibition in advanced Merkel cell carcinoma

Ivelina Spassova ,[1,2] Selma Ugurel ,[2] Linda Kubat,[1,2] Lisa Zimmer,[2] Patrick Terheyden ,[3] Annalena Mohr,[3] Hannah Björn Andtback,[4] Lisa Villabona,[4] Ulrike Leiter,[5] Thomas Eigentler,[5] Carmen Loquai,[6] Jessica C Hassel,[7,8] Thilo Gambichler,[9] Sebastian Haferkamp,[10] Peter Mohr,[11] Claudia Pfoehler,[12] Lucie Heinzerling,[13] Ralf Gutzmer,[14] Jochen S Utikal,[8,15] Kai Horny,[1,8,16] Hans-Ulrich Schildhaus,[17] Daniel Habermann,[18] Daniel Hoffmann,[18] Dirk Schadendorf,[2,16] Jürgen Christian Becker [1,2,8,16]

To cite: Spassova I, Ugurel S, Kubat L, *et al*. Clinical and molecular characteristics associated with response to therapeutic PD-1/PD-L1 inhibition in advanced Merkel cell carcinoma. *Journal for ImmunoTherapy of Cancer* 2022;**10**:e003198. doi:10.1136/jitc-2021-003198

► Additional supplemental material is published online only. To view, please visit the journal online (http://dx.doi.org/10.1136/jitc-2021-003198).

IS and SU contributed equally.

Accepted 11 December 2021

For numbered affiliations see end of article.

Correspondence to
Professor Jürgen Christian Becker; j.becker@dkfz.de

ABSTRACT

Background Based on its viral-associated or UV-associated carcinogenesis, Merkel cell carcinoma (MCC) is a highly immunogenic skin cancer. Thus, clinically evident MCC occurs either in immuno-compromised patients or based on tumor-intrinsic immune escape mechanisms. This notion may explain that although advanced MCC can be effectively restrained by treatment with PD-1/PD-L1 immune checkpoint inhibitors (ICIs), a considerable percentage of patients does not benefit from ICI therapy. Biomarkers predicting ICI treatment response are currently not available.

Methods The present multicenter retrospective study investigated clinical and molecular characteristics in 114 patients with unresectable MCC at baseline before treatment with ICI for their association with therapy response (best overall response, BOR). In a subset of 21 patients, pretreatment tumor tissue was analyzed for activation, differentiation and spatial distribution of tumor infiltrating lymphocytes (TIL).

Results Of the 114 patients, n=74 (65%) achieved disease control (BOR=complete response/partial response/stable disease) on ICI. A Bayesian cumulative ordinal regression model revealed absence of immunosuppression and a limited number of tumor-involved organ systems was highly associated with a favorable therapy response. Unimpaired overall performance status, high age, normal serum lactate dehydrogenase and normal serum C reactive protein were moderately associated with disease control. While neither tumor Merkel cell polyomavirus nor tumor PD-L1 status showed a correlation with therapy response, treatment with anti-PD-1 antibodies was associated with a higher probability of disease control than treatment with anti-PD-L1 antibodies. Multiplexed immunohistochemistry demonstrated the predominance of $CD8^+$ effector and central memory T cells (T_{CM}) in close proximity to tumor cells in patients with a favorable therapy response.

Conclusions Our findings indicate the absence of immunosuppression, a limited number of tumor-affected organs, and a predominance of $CD8^+$ T_{CM} among TIL, as baseline parameters associated with a favorable response to PD-1/PD-L1 ICI therapy of advanced MCC. These factors should be considered when making treatment decisions in MCC patients.

INTRODUCTION

Merkel cell carcinoma (MCC) is a rare, highly aggressive neuroendocrine skin cancer. MCC carcinogenesis is associated either with the Merkel cell polyomavirus (MCPyV), predominantly in cases occurring in the northern hemisphere, or with chronic UV-exposure.[1] MCC is highly immunogenic due to the presence of either MCPyV-derived antigens or UV-associated neoantigens. Thus, clinically manifest advanced MCC is mostly observed in immunocompromised and immunosenescent patients or occurs based on tumor-intrinsic immune escape mechanisms. Still, a high therapeutic activity of PD-1/PD-L1 immune checkpoint inhibitors (ICIs) with durable objective responses in about 50% of patients has been observed.[2] Despite this major improvement in the therapy outcome of advanced MCC patients, this observation also implies that half of the patients do not experience a long-term benefit from ICI therapy. Clinically applicable predictive biomarkers of ICI therapy response are just starting to emerge: (1) in a trial testing neoadjuvant nivolumab, both pathological complete response (CR) and radiographic tumor regression at the time of surgery were correlated with improved recurrence-free survival,[3] and (2) Kacew *et al* reported that a limited disease stage at ICI therapy start was associated with a favorable response.[4]

However, the study also showed that, unlike in other cancers, neither tumor mutational burden nor copy-number alterations in MCC tumor tissue predicted ICI therapy outcome. Similarly, a recent study by us characterizing 41 MCC patients receiving PD-1/PD-L1 ICI demonstrated that predictive markers of ICI therapy response established in other cancer entities such as neutrophil-to-lymphocyte ratio, metastatic stage and site of the primary were not associated with ICI response in MCC.[5] However, our comprehensive dynamic molecular analysis of pretreatment tumor tissue demonstrated that not only the density of the immune cell infiltrate, but rather its functional properties correlated with the response to ICI therapy. In particular, the predominance of central memory T (T_{CM}) cells with a diverse T-cell receptor (TCR) repertoire were associated with a favorable treatment outcome.[5] On the other hand, we did not observe any predictive potential on previously suggested molecular biomarkers such as tumor PD-L1 expression or MCPyV status.[2 5 6] Thus, with the present study we aimed at testing clinically well applicable predictive biomarkers in a larger patient cohort (114 MCC patients, although these included 41 patients from our earlier study[5] by expanding our initial oligocentric approach to a multicentric study, but also limiting the complexity of the molecular analyses to those showing the highest predictive value in our previous study.

MATERIALS AND METHODS

Patients and samples

One hundred and fourteen (n=114) patients treated between May 2018 and July 2020 at 11 MCC referral centers (Bochum, Buxtehude, Erlangen, Essen, Heidelberg, Homburg, Lübeck, Mainz, Regensburg, Stockholm, Tübingen) were retrospectively identified according to the following selection criteria: histopathologically confirmed diagnosis of MCC, treatment with PD-1/PD-L1 ICI for unresectable advanced disease, and complete follow-up documentation of ICI therapy outcome including best overall response (BOR), progression-free (PFS) and overall (OS) survival. BOR was determined according to RECIST V.1.1.[7] PFS and OS were defined as time from therapy start until disease progression or death, respectively; if no such event occurred, the date of the last patient contact was used as endpoint of survival assessment (censored observation). Detailed clinical parameters at baseline of ICI therapy were collected from the patients' medical charts; it is important to note that a subgroup of 41 patients had already been described in an earlier study[5] (online supplemental table S1). Immunosuppression was assigned to patients suffering from hematological neoplasia or to patients treated with multiple drugs for multiple cancers or immunosuppressive medications. If available, pretreatment samples of formalin-fixed paraffin-embedded (FFPE) tumor tissue from the studied patients were collected for molecular analysis.

Detection of MCPyV DNA

Detection of MCPyV DNA was performed as previously described by TaqMan Real-Time qPCR using the following large T-antigen (LTA) specific primers and TaqMan probe: forward primer; CCA AAC CAA AGA ATA AAG CAC TGA; reverse primer, TCG CCA GCA TTG TAG TCT AAA AAC, and probe: FAM-AGC AAA AAC ACT CTC CCC ACG TCA GAC AG-BHQ1.[5]

Multiplex immunofluorescence staining

Multiplex immunofluorescence staining of FFPE tumor tissue was performed using the Opal chemistry (PerkinElmer, Waltham, USA, Cat.No.: OP7TL4001KT) with two panels of antibodies, ie, against CD4, CD8, CD20, Foxp3 and CD68 (panel 1), or CD27, GZMB, TCF1, CD45RA and CD45RO (panel 2). Synaptophysin served as tumor marker in either panels. Briefly, after deparaffinization and fixation, 3 µm tumor sections were processed with retrieval buffers for 15 min in an inverter microwave oven. Thereafter, sections were incubated with the antibody diluent for 10 min at room temperature, followed by incubation with the primary antibody for 30 min. After applying Opal polymer HRP secondary antibody and Opal fluorophore solution each for 10 min, antibodies were removed by microwave treatment before a further round of staining. The antibodies, their dilutions, the respective retrieval buffers as well as the sequence of usage are described in detail in online supplemental table S2. Visualization of the different fluorophores was achieved on the Mantra Quantitative Pathology Imaging System (PerkinElmer). For each tumor sample, quantification of the different cell types was performed at medium magnification on three randomly selected areas located either in the juxtatumoral or intratumoral region in a semiautomatic fashion with the InForm Tissue Analysis software (Akoya Biosciences, Menlo Park, USA). Since tumor samples were received from different pathology institutes, the quality of the FFPE material was not uniform, resulting in variations in fluorescence intensity from sample to sample. To avoid quantification errors due to these intensity variations, the InForm tissue analysis software was trained on tumor tissue samples from the respective sources, thus developing an algorithm based on the median of the determined intensities. Subsequently, training of the software was performed on five different MCC tissue samples to recognize staining patterns/cell types. Finally, a principal components analysis was used to visualize possible pattern of the immunofluorescence staining results across the samples as suggested by Shen *et al*.[8] Annotation by the different pathology institutes the samples were received from no significant batch effect was observed indicating the initial training of the InForm software was sufficient.

Two independent observer, blinded to ICI response, monitored the quantification analysis and classified the respective cell types in relation to all nucleated cells per sample into five categories: 0%, >1%, 1%–5%, 5%–10% and >10%. Disagreements were resolved by

taking the opinion of a third observer into consideration. Markers used for the quantification of the different immune cell types are listed in online supplemental table S3 and the raw data of the quantification analysis by InForm Tissue Analysis software is provided in online supplemental table S4 and S5 for panel 1 and panel 2, respectively.

STATISTICAL ANALYSES

A Bayesian cumulative ordinal regression model was applied for predicting PD-1/PD-L1 ICI therapy response in MCC patients. The model was fit with a dataset consisting of 114 patients and 15 clinical parameters; year of treatment and participation in a clinical trial were considered as possible confounders (table 1). Model parameters were described with probability distributions that take into account the uncertainty of the estimates. Treatment response was classified into CR, partial response (PR), stable disease (SD) and progressive disease (PD) on an ordinal scale. We applied a cumulative ordinal regression model to the data, which takes the ordinal nature of the response variable into account. Compared with other approaches that incorrectly treat the response variable as metric (such as linear regression) or nominal (eg, by binarizing the response variable), this may lead to more precise inference and therefore reduces over- or underestimation of effect sizes.[9] The cumulative regression model regards the tendency of a patient to respond to treatment as a latent (=unobserved) variable that is determined by the patient characteristics. The model is described by the following formula: $_i = \beta_{age}.x_{i,age} + \beta_{LDH}.x_{i,LDH} \ldots .$; in which is the location of the latent variable for patient i, β_{age} is the β coefficient for the predictor age and $x_{i,age}$ is the indicator variable of patient i for age. The β coefficient of the predictor provides information on whether or not a predictor is associated with a higher probability of treatment response. Student t-priors with 7 degrees of freedom and a SD of 1 were chosen as weakly informative priors for the β coefficients. Model fit is performed numerically by Markov chain Monte Carlo.[10] The width of the distribution gives an impression of the uncertainty of the estimate: a distribution tightly concentrated around a value means that the dataset allows for a precise estimate of that parameter, while a broader distribution means that the data is consistent with a wide range of parameter values. Average predictive comparisons are calculated as expected changes in response associated with a unit difference in one of the inputs. They were calculated with respect to having at least a PR to treatment, for example, for immunosuppression, values between −0% and −40% denote that comparing a patient with immunosuppression to an otherwise identical patient without immunosuppression, the patient with immunosuppression has (on average) a 0%–40% lower probability of having at least a PR to treatment. Fitting the model to the dataset was done with the R software package 'brms', which utilizes 'Stan' in the background.[11] Missing values were estimated by multiple imputation with the R package 'mice'.[11–13] The imputed data values are consistent with the observed data (online supplemental figure 1). Using leave-one-out cross-validation (LOO), this model has a similar (expected log-predictive density (ELPD), a measure of its ability to generalize to unseen data) as a sequential model without category-specific effects, meaning that including category-specific effects does not improve model performance and the proportional odds assumption does not have a strong effect on the model conclusions. In the following, we report the detailed results for LOO and ELPD for completeness (online supplemental figure 2). A detailed description is given in online supplemental materials and methods. Transparent Reporting of a multivariable prediction model for Individual Prognosis or Diagnosis reporting guidelines were followed to develop the predictive model, including patient selection.[14]

Kaplan-Meier plots were generated with R V.3.5.1 using the package 'survival' (V.2.44–1.1 and survminer V.0.4.6). All patients with PFS and/or OS of more than 36 months are censored without having a respective event, because the data beyond this period is very sparse. Log rank test is used to calculate p values.

For statistical testing of T-cell abundance in MCC tumor tissue, p values were determined by beta regression with R V.4.0.2 and packages 'lmtest' and 'betareg' (V.0.9–38 and V.3.1–4).

For statistical testing of the distance between tumor cells and $CD8^+$ T cells in tumor tissue, the unpaired two-tailed Student's t-test, calculated in GraphPad Prism V.5 (San Diego, USA) was applied.

RESULTS

Patient characteristics, response to ICI and survival outcomes

A total of 114 patients treated with PD-1/PD-L1 ICI (avelumab, n=57; nivolumab, n=13; pembrolizumab, n=44) for unresectable advanced MCC were identified at 11 MCC referral centers in Germany and Sweden. Detailed patient characteristics are given in table 1. Of 114 patients, 54 (47%) experienced an objective response (BOR=CR/PR), and 74/114 patients (65%) a disease control (BOR=CR/PR/SD) on ICI (figure 1A). When the entire patient cohort was divided by type of therapy, in the cohort treated with the anti-PD-L1 antibody avelumab, 22/57 patients (39%) experienced an objective response and 33/57 patients (58%) disease control; in the cohort treated with the anti-PD-1 antibodies pembrolizumab or nivolumab, an objective response was observed in 32/57 patients (56%) and disease control in 41/57 patients (72%). Of 114 patients, 37 (32%) died within a median follow-up time of 12.0 (±2.41, 95% CI) months. Kaplan-Meier estimates for PFS and OS categorized by BOR (CR, n=24; PR, n=30; SD, n=20; and PD, n=40) revealed a clear separation of the curves for patients experiencing disease control (CR/PR/SD) as BOR compared with those presenting a primary progression on therapy (online supplemental figure 3). The median PFS and OS in the

Table 1 Patient and tumor characteristics at baseline of anti-PD-1/PD-L1 therapy

	All patients n=114 (100%)	Disease control (BOR=CR/PR/SD) n=74 (100%)	Disease progression (BOR=PD) n=40 (100%)
Patient characteristics			
Gender			
Male	82 (72%)	54 (73%)	28 (70%)
Female	32 (28%)	20 (27%)	12 (30%)
Age			
<70	40 (35%)	24 (32%)	16 (40%)
≥70	74 (65%)	50 (68%)	24 (60%)
Overall performance status (ECOG)			
0	64 (56%)	47 (64%)	17 (43%)
≥1	49 (43%)	26 (35%)	23 (57)
Not available	1 (1%)	1 (1%)	0 (0%)
Immunosuppression			
No	92 (81%)	64 (86%)	28 (70%)
Yes	22 (19%)	10 (14%)	12 (30%)
LDH (blood)			
Normal	43 (38%)	32 (43%)	11 (28%)
Elevated	67 (59%)	39 (53%)	28 (70%)
Not available	4 (3%)	3 (4%)	1 (2%)
CRP (blood)			
Normal	30 (26%)	21 (28%)	9 (23%)
Elevated	55 (48%)	31 (42%)	24 (60%)
Not available	29 (26%)	22 (30%)	7 (16%)
NLR (blood)			
<4	54 (47%)	36 (49%)	18 (45%)
≥4	35 (31%)	20 (27%)	15 (38%)
Not available	25 (22%)	18 (24%)	7 (17%)
Tumor characteristics			
Localization of primary			
Head and neck	24 (21%)	17 (23%)	7 (17%)
Extremities	44 (39%)	27 (36%)	17 (43%)
Trunk	19 (17%)	12 (16%)	7 (17%)
Unknown primary	15 (13%)	9 (12%)	6 (15%)
Metastatic stage (AJCC)			
M0	17 (15%)	11 (15%)	6 (15%)
M1a	36 (32%)	23 (31%)	13 (32%)
M1b/M1c	61 (53%)	40 (54%)	21 (53%)
Organs involved			
1	51 (45%)	38 (51%)	13 (32%)
>1	63 (55%)	36 (49%)	27 (68%)
MCPyV status (tumor)			
Negative	10 (9%)	6 (8%)	4 (10%)
Positive	32 (28%)	20 (27%)	12 (30%)
Not available	72 (63%)	48 (65%)	24 (60%)
PD-L1 (tumor)			
Negative	17 (15%)	11 (15%)	6 (15%)

Continued

Table 1 Continued

	All patients n=114 (100%)	Disease control (BOR=CR/PR/SD) n=74 (100%)	Disease progression (BOR=PD) n=40 (100%)
Positive	21 (18%)	12 (16%)	9 (23%)
Not available	76 (67%)	51 (69%)	25 (62%)
Therapeutic interventions			
Previous radiotherapy			
No	55 (48%)	35 (47%)	20 (50%)
Yes	59 (52%)	39 (53%)	20 (50%)
Previous chemotherapy			
No	83 (73%)	53 (72%)	30 (75%)
Yes	31 (27%)	21 (28%)	10 (25%)
PD-1/PD-L1 inhibitor therapy			
Avelumab	57 (50%)	33 (45%)	24 (60%)
Nivolumab	13 (11%)	10 (13%)	3 (8%)
Pembrolizumab	44 (39%)	31 (42%)	13 (32%)

AJCC, American Joint Committee on Cancer; BOR, best overall response; CRP, C reactive protein; ECOG, Eastern Cooperative Oncology Group; LDH, lactate dehydrogenase; MCPyV, Merkel cell polyomavirus; NLR, neutrophil to lymphocyte ratio.

control group were 12.1 and 15.9 months, and 1.4 and 3.9 months, respectively, in the progression group.

On the finding of this clear separation in survival probabilities between patients responding with disease control (BOR=CR/PR/SD) and patients responding with disease progression (BOR=PD), we performed all further molecular analyses on the association of clinical and molecular characteristics with therapy response based on the discrimination between these two patient groups (ie, disease control group vs disease progression group). Due to the limited number of samples, we refrained from forming further subclusters taking the degree of response into account.

Baseline clinical parameters are associated with a favorable response to ICI therapy

Most predictive models dichotomize response to therapy, which neglects the extent of the response. To overcome this limitation, we developed a Bayesian model that instead of dichotomizing the therapy response into two groups, *that* is, regression *versus* progression, rather reflects the established clinical response evaluation

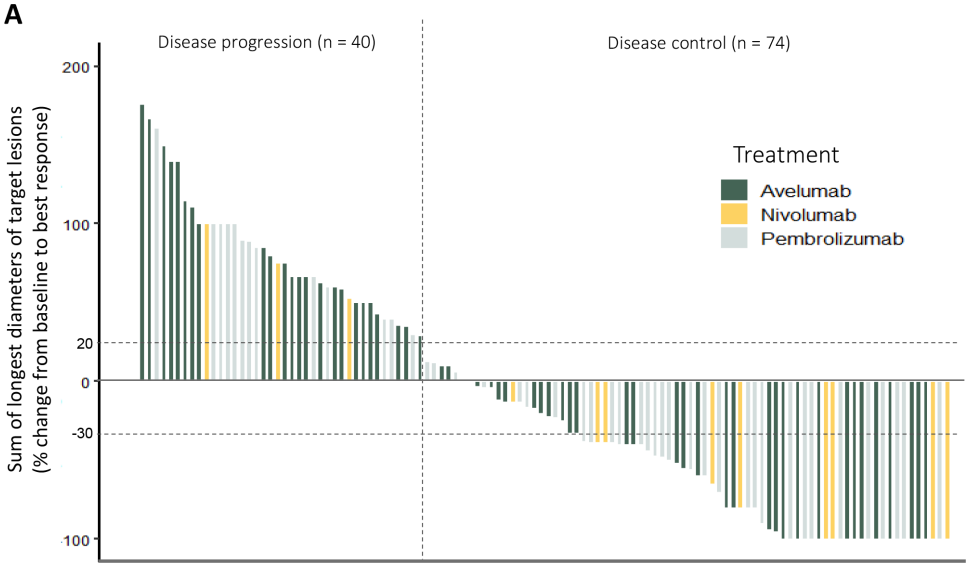

Figure 1 Response of n=114 advanced MCC patients on PD-1/PD-L1 immune checkpoint inhibition therapy. Waterfall plot depicting the best overall response (BOR) as change in the sum of the longest diameters of target lesions from baseline to BOR. Each bar, color coded by therapeutic antibody, represents an individual patient. The pointed vertical line discriminates patients with disease control (BOR=CR/PR/SD) from patients with disease progression (BOR=PD). CR, complete response; MCC, Merkel cell carcinoma; PD, progressive disease; PR, partial response; SD, stable disease.

criteria in solid tumors (RECIST): CR, PR, SD, and PD.[7] Resulting from this Bayesian model, we found the absence of immunosuppression as well as a limited number of organs (1 vs>1) involved into disease spread as the strongest predictors of a favorable response to PD-1/PD-L1 ICI therapy (figure 2). Interestingly, the involved organ type, for example, soft tissue versus visceral, showed less predictive power. These calculations indicate that immunocompetent patients or patients with only one affected organ have probability to achieve disease control on ICI treatment, that is by about 20% higher (0%–40% increase contains almost all the probability). Additionally, an unimpaired overall performance status (Eastern Cooperative Oncology Group (ECOG)=0), patient age of 70 years and above, as well as normal lactate dehydrogenase (LDH) and C reactive protein (CRP) serum levels were associated with a higher probability of disease control on ICI, but to a lower extent. Interestingly, patients' sex, localization of the primary, pretreatment with radiation or chemotherapy, and MCPyV status or PD-L1 expression of the tumor revealed no relevant association with ICI therapy response. Similarly, when we tested if year of treatment and participation in a clinical trial were possible confounders, no impact on the therapeutic outcome was observed. Surprisingly, in our investigated patient cohort with an equal distribution of PD-L1 and PD-1 ICI therapies (see table 1), the use of anti-PD-1 antibodies for ICI therapy was associated with a higher probability of a favorable therapy response (figure 2). Notably, the distribution of relevant patient and tumor characteristics, particularly immunosuppressive state, number of organs involved with disease, impaired ECOG status, and elevated serum LDH and CRP were equally distributed among the two treatment cohorts, that is, anti-PD-1 and anti-PD-L1 antibody ICI (online supplemental table S6).

Pretreatment dense intratumoral infiltrates of CD8$^+$ T_{CM} are associated with a favorable response to ICI

We recently demonstrated by transcriptomics, spatial proteomics and TCR sequencing of sequential tumor biopsies under PD-1/PD-L1 ICI therapy that a predominance of T_{CM} with a diverse TCR repertoire and the ability to expand on ICI is associated with a favorable therapy response.[5] This approach allows a good understanding of the complex immune biology of MCC, but is difficult to use in the clinical routine of patient care. In order to establish clinically well applicable predictive biomarkers, we here limited the complexity of our molecular investigations to multiplexed immunohistochemistry of pretreatment FFPE tumor tissue in order to extract the most important cell type characteristics for therapy response, which can be realistically analyzed as predictive biomarker in the future. Phenotyping of the immune infiltrate of pretreatment tumor tissue samples of 21 patients, including some tumors from our earlier report,[5] (11 patient with disease control, 10 patients with disease progression) for the expression of CD4, CD8, CD20, Foxp3, and CD68 showed that dense immune cell infiltration, particularly by CD8$^+$ T cells, correlated with a favorable ICI therapy response (figure 3A,B). Significantly more CD8$^+$ T cells were infiltrating the juxtatumoral area (p=0.02) and higher number of cytotoxic T cells were present in the intratumoral area (p=0.16) of patients achieving disease control (figure 3C, online supplemental figure 4). Figure 3D illustrates how the spatial distribution of the tumor-infiltrating CD8$^+$ T cells was measured as the distance between the nuclei of CD8$^+$ T cells and synaptophysin$^+$ MCC cells. For distance analysis, tumor samples with CD8$^+$ T cells that were less than 1% of total cells had to be excluded, because in these cases it was not possible to measure the distance of at least 20 different tumor/T–cell pairs. In patients with disease control, CD8$^+$ T cells were in direct and close contact with the tumor cells with a mean distance length of 13.24 µm, whereas the mean distance length was significantly higher in patients with disease progression (22.00 µm, p=0.009) (figure 3E). Moreover, in patients showing disease progression, the CD8$^+$ T cells were mostly restricted to the juxtatumoral stromal space, and only rarely within the tumor tissue. We did not detect significant differences in the amount or distribution of regulatory T cells (CD4$^+$FoxP3$^+$), B cells (CD20$^+$), and monocytes/macrophages (CD68$^+$) between tumor tissues of patients with disease control and patients with disease progression. However, with respect to CD20$^+$ B cells within the cellular immune infiltrate, it is important to note that their frequency varied strongly between samples.

Staining for CD27, GZMB, TCF1, CD45RA and CD45RO allows a precise distinction of T_{CM} and effector T cells with T_{CM} characterized by colocalization of CD27, TCF1 and CD45RO. Indeed, only in pretreatment tumors from patients with disease control, we observed a clear co-localization of these T_{CM} markers (figure 4). Moreover, quantification of T-cell subtypes confirmed a higher percentage of T_{CM} of total tumor infiltrating lymphocytes (TILs) number in the intratumoral infiltrate as well as in the juxtatumoral area (table 2). Effector T cells characterized by colocalization of GZMB and CD45RA were also more frequently observed in the cellular tumor infiltrate of pretreatment tumor tissue of patients with disease control than in those with disease progression; however, the difference was less evident (p=0.07; online supplemental figure 5). It should be noted that CD45RA re-expression has also been described in terminally differentiated T cells characterized by decreased proliferative capacity, increased senescence signaling in vitro.[15]

DISCUSSION

To find predictors, which assess the individual probability of success of PD-1/PD-L1 ICI in MCC, we collected clinical information on 114 accordingly treated patients and established the spatial distribution of tumor infiltrating T cells as well as their activation and differentiation status in pretreatment FFPE tumor tissue samples by two IHC panels. We developed a Bayesian cumulative ordinal

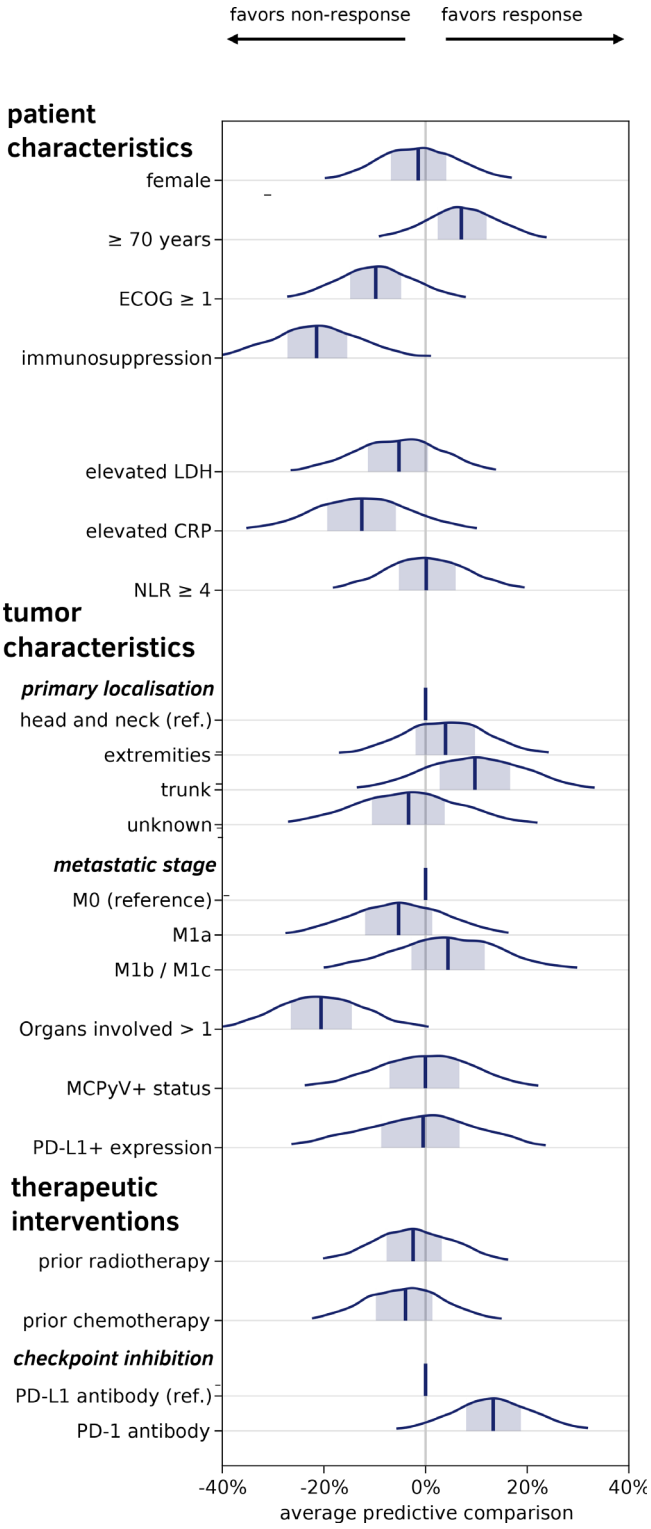

Figure 2 Best overall response (BOR) to anti-PD-1/PD-L1 therapy in correlation to baseline clinical patient and tumor characteristics. The correlations are visualized by average predictive comparisons calculated by a Bayesian cumulative ordinal regression model. While the presented data refer to the full model using four categories of response: CR, PR, SD, and PD, to ease interpretation we mapped the obtained results by average predictive comparisons on a single probability scale for disease control (BOR=CR/PR/SD) and disease progression (BOR=PD) as a probability distribution, given as the percentage of average predictive comparison. The 95% credibility intervals are colored in light blue. Distinct parameters are marked as reference (Ref), described as vertical blue lines set at 0% average predictive comparison. CR, complete response; CRP, C reactive protein; ECOG, Eastern Cooperative Oncology Group; LDH, lactate dehydrogenase; MCPyV, Merkel cell polyomavirus; NLR, neutrophil to lymphocyte ratio; PD, progressive disease; PR, partial response; SD, stable disease.

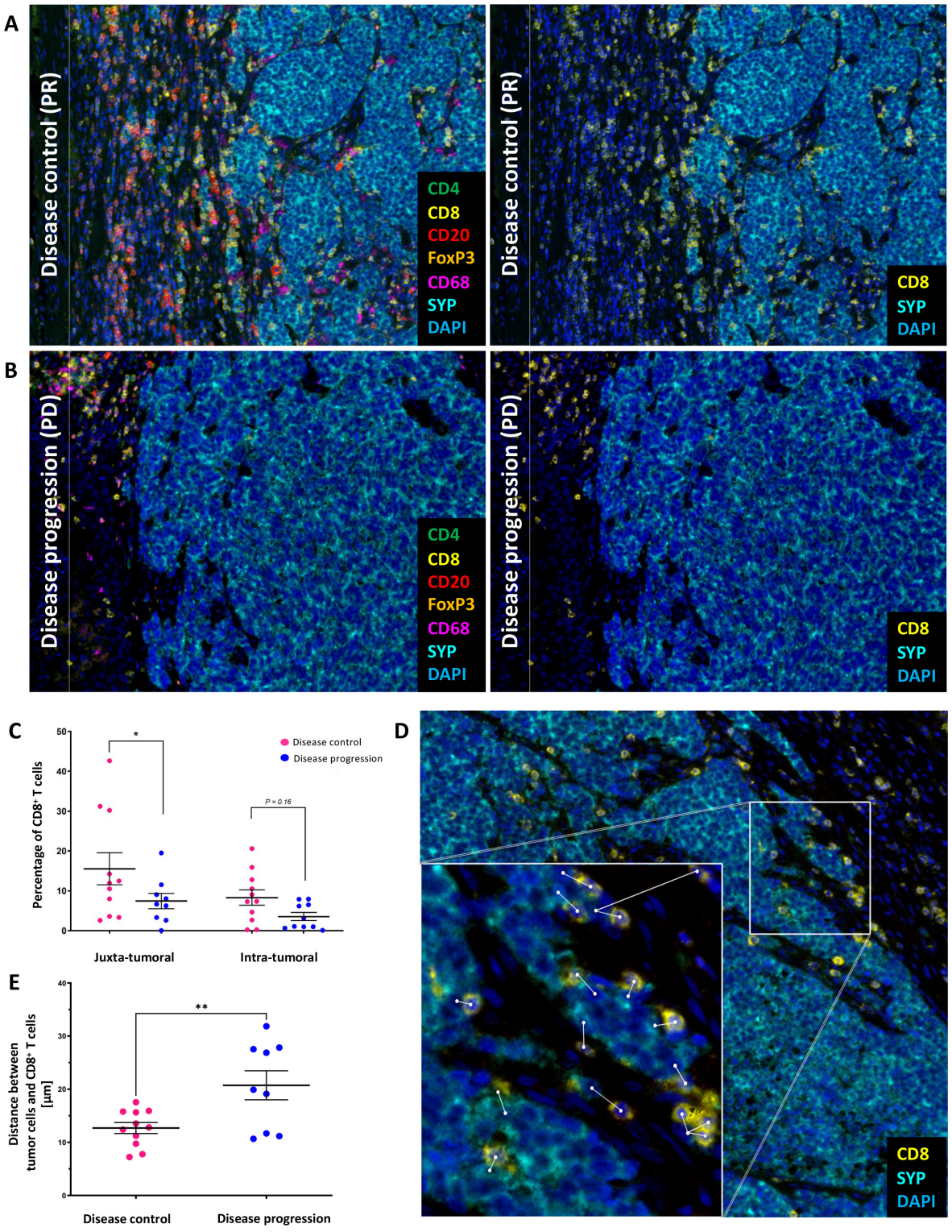

Figure 3 High density of tumor-infiltrating CD8$^+$ central memory T cells in close proximity to tumor cells in MCC patients showing disease control (CR/PR/SD) on PD-1/PD-L1 ICI phenotyping of the cellular immune infiltrate present in MCC tumor lesions obtained at baseline of ICI therapy of a representative patient responding with disease control (A) and disease progression (B) was done by multiplexed immunohistochemistry-based staining using antibodies against CD4 (green), CD8 (yellow), CD20 (red), FOXP3 (orange), CD68 (magenta), and the MCC marker synaptophysin (SYN) (cyan); nuclei are stained with DAPI (blue). depicted are merged images at ×20 magnification. (C) Percentage of CD8$^+$ T cells in pretreatment tumor tissue from patients showing disease control and those showing disease progression in the juxtatumoral and intratumoral area. P values were determined using beta regression. (D) Measurement of the distance between CD8$^+$ T cells and tumor cells. (E) Mean value of the distance between CD8$^+$ T cells and tumor cells for patients showing disease control and those showing disease progression. P values were determined using unpaired, two-tailed Student's t-test. CR, complete response; ICI, immune checkpoint inhibitor; MCC, Merkel cell carcinoma; PR, partial response; SD, stable disease.

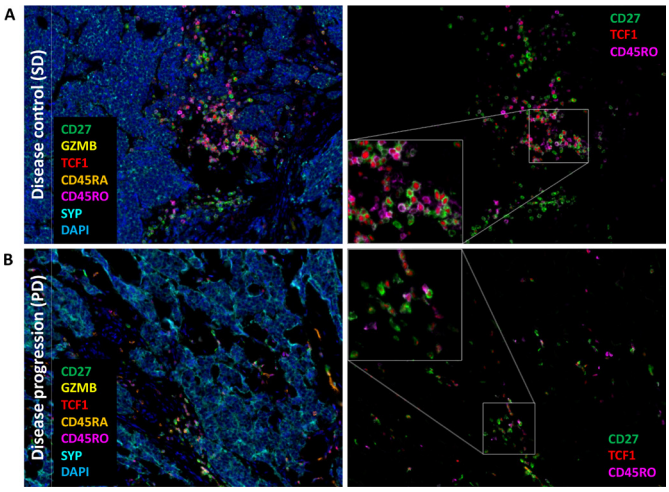

Figure 4 Predominance of central memory T cells (T_{CM}) among tumor-infiltrating lymphocytes of patients showing disease control (CR/PR/SD) on PD-1/PD-L1 ICI therapy. Multiplexed immunofluorescence staining of pretreatment tumor tissue from a representative patient showing disease control (A) and disease progression (B) using antibodies against CD27 (green), GZMB (yellow), TCF1 (red), CD45RA (orange), CD45RO (magenta), and the MCC marker synaptophysin (SYN) (cyan); nuclei are stained with DAPI (blue). Depicted are merged images at ×20 magnification. To visualize the colocalization of CD27, TCF1 and CD45RO, an enlarged image view is shown. CR, complete response; ICI, immune checkpoint inhibitor; MCC, Merkel cell carcinoma; PR, partial response; SD, stable disease.

regression model that includes the distance between clinical characteristics and thereby appropriately accounts for category order. This model avoids problems such as dichotomizing the outcome or treating the distance between the categories as equal, and thus uses the available data efficiently. It revealed the absence of immunosuppression and the metastatic involvement of a limited number of organ systems as characteristics predicting disease control on PD-1/PD-L1 ICI therapy with the highest probability. Additional characteristics associated with treatment response were age, overall performance status, serum LDH and serum CRP, as well as a brisk intratumoral infiltrate by T_{CM} (figure 5). However, both the data model and the missing data model rely on assumptions about the data generating process, for example, that data are missing at random. Even if the implications of these assumptions have been evaluated carefully, all results are still conditioned on the underlying model and should be interpreted with this in mind.

The expanded patient cohort under investigation of n=114 that allowed fitting a more complex Bayesian model supported our previously published observations in 41 patients.[5] The positive effect of an intact immune system observed in either study was also reported from the avelumab expanded access program for metastatic MCC patients in which immunocompromised patients achieved a lower response rate with shorter durations of response.[16] It should be noted that other characteristics associated with a lower probability of response, such as a limited performance status (ECOG >0) or an elevated serum CRP, are also likely to reflect an impaired immune status of the respective patient. Similarly, an elevated serum LDH level and a higher number of involved organs are not to be interpreted only as markers of a higher tumor load. Notably, in our previous report, we dichotomized the number of involved organs up to two or more, these groups did not show a clear association with the probability of response but had broad posterior intervals; in contrast, the larger cohort is consistent with the involvement of only one organ being a strong positive predictive marker. Patient age of 70 years and above was also found to be associated with a higher probability of disease control, but to a lesser extent. A positive correlation of response to anti-PD-1 therapy and patient age ≥60 years was described in melanoma.[17] In this respect, it is important to note that chronological age does not necessarily reflect immunological age. One factor that correlates better with biological/immunological age than chronological age is frailty, which directly describes a person's health status.[18] For example, the process of inflammation is a predictor for frailty and one of the key cell types believed to facilitate an inflammatory phenotype are tumor-infiltrating macrophages, which are often detected in MCC tissue.[19] Other clinical characteristics such as sex, primary site, prior radiation or chemotherapy, PD-L1 expression by tumor cells, and tumor MCPyV status did not show relevant association to PD-1/PD-L1 ICI response. These observations are in line with the results from a study scrutinizing 37 MCC patients receiving ICI.[20]

Functional characterization of the immunological infiltrate of pretreatment tumor tissue revealed that in particular the presence of T_{CM} in close proximity to tumor cells was associated with a favorable response to ICI therapy. It is important to note that because the tumor samples were received from different pathology institutes, the quality of the FFPE material was not uniform, resulting in variations in fluorescence intensity from sample to sample. To avoid quantification errors due to these intensity variations, the InForm tissue analysis software was trained on tumor tissue samples from the respective sources, thus developing an algorithm based on the median of the determined intensities. Moreover, the observation was consistent with our previous work, where we performed transcriptomics, spatial proteomics and TCR sequencing of sequential tumor biopsies before and under ICI therapy of rather uniform quality. These observations confirm the robustness of the chosen approach and the importance of T_{CM} as one of the effectors of response to ICI therapy. The superior antitumor efficacy of T_{CM} cells can be explained by their low activation threshold, rapid proliferative and differentiation capacity on cognate activation, as well as their capacity for long-term persistence facilitating immunologic memory.[21 22] Indeed, since T_{CM} cells are the major source of secondary effector cells during a recall response, the duration of anti-tumor immune responses depends

Table 2 Quantification of the cellular tumor infiltrate characterized by multiplex immunohistochemistry staining

Pretreatment MCC tumor tissue samples

Response to CPI		Total leucocyte no per observed area		T_{CM} in % of total lymphocyte no per observed area	
		Juxtatumoral	Intratumoral	Juxtatumoral	Intratumoral
Disease control	PR	2121	731	4.7	2.2
	CR	1510	989	3.0	2.7
	CR	1813	3519	0.0	22.0
	SD	5436	9405	18.0	11.7
	PR	1902	2162	6.7	8.0
	PR	1451	97	13.0	26.7
	SD	115	283	23.0	33.0
	CR	1	14	0.0	0.0
	PR	1846	6030	0.0	11.0
	PR	1681	2080	13.0	11.7
	CR	2261	428	33.0	36.7
	Mean value	1831	2340	10.4	15.1
Disease progression	PD	*NA*	0	*NA*	0.0
	PD	44	54	0.0	0.0
	PD	1125	124	0.0	0.0
	PD	239	170	12.0	15.0
	PD	3831	2478	22.0	13.0
	PD	316	376	17.0	10.0
	PD	0	13	0.0	0.0
	PD	2438	287	3.7	0.5
	PD	403	62	2.0	1.7
	PD	159	66	0.0	0.0
	Mean value	950	363	6.3	4.0

Tumor tissue samples were obtained from MCC patients prior to the start of PD-1/PD-L1 immune checkpoint inhibitor therapy. Lymphocytes were identified based on $CD45RA^+$ or $CD45RO^+$ staining and the sum of both signals were used for the quantification of the total lymphocyte number per sample per observed area. T_{CM} were determined based on the triple $CD27^+TCF1^+CD45RO^+$ staining.
CPI, checkpoint inhibition; CR, complete response; MCC, Merkel cell carcinoma; PD, progressive disease; PR, partial response; SD, stable disease; T_{CM}, central memory T-cells.

on their presence.[23] This is consistent with our present and recent findings as well as with further studies showing T_{CM} characteristics to be effectively reactivated.[24–27] Toews *et al* demonstrated that T_{CM}-derived CAR T cells showed an augmented antitumor immunity against neuroblastoma cells under PD-1 blockade and subsequently formed

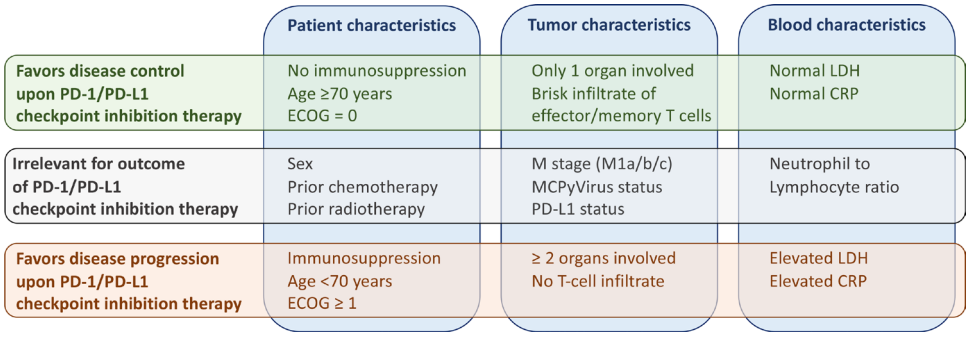

Figure 5 Schematic overview on relevant clinical and molecular parameters determined before treatment and their predictive value on PD-1/PD-L1 ICI therapy response. CRP, C reactive protein; ECOG, Eastern Cooperative Oncology Group; ICI, immune checkpoint inhibitor; LDH, lactate dehydrogenase.

a resident memory T-cell subset following tumor challenge.[28] In non-small cell lung cancer patients treated with nivolumab, a longer PFS was observed in patients with a high T_{CM}/T_{EFF}-cell ratio in the circulation, suggesting an enrichment of peripheral circulating T_{CM} subpopulations also as a potential positive predictive marker.[29] Similarly, in hepatocellular carcinoma patients, according to midterm clinical trial results, an extended median relapse-free survival was associated with an increased T_{CM}-subpopulation.[22] Moreover, Siddiqui *et al* reported the presence of a $TCF1^+PD\text{-}1^+CD8^+$ T-cell subpopulation in the circulation of melanoma patients and among TILs of primary melanomas. In conclusion, the success of PD-1/PD-L1 ICI therapy seems not to depend on the rejuvenation of differentiated exhausted T cells, but rather on the proliferation of the less-differentiated memory-like $CD8^+$ T cells.[30]

Long-lived memory T-cell formation and maintenance are driven by transcription factors like FOXO1, EOMES and TCF1. In particular, TCF1 was identified as the master regulator of genes, inducing serial T-cell reactivation and self-renewal. With respect to the limited predictive value of the presence of granzyme-expressing T cells in the tumor infiltrate, recently a granzyme-positive subpopulation of $CD8^+$ T cells associated with age-related dysfunction of the immune system has been described.[31] These cells are characterized by a pronounced tissue-homing capacity and a high clonality, that is, expressing only a limited diversity of TCRs, which might be of particular relevance for MCC, since this tumor affects mainly the elderly population. Indeed, we have shown in previous studies that high clonality of TIL in MCC is both a negative prognostic and predictive biomarker.[5 32]

In conclusion, our results provide a number of clinically well applicable baseline biomarkers associated with PD-1/PD-L1 ICI therapy response in patients suffering from advanced MCC. On a functional level, we confirmed the predominance of T_{CM} among TILs in patients with a favorable ICI therapy response; a factor which can be determined on FFPE tissue.

Author affiliations
[1]Translational Skin Cancer Research, Deutsches Konsortium für Translationale Krebsforschung, Essen, Germany
[2]Department of Dermatology, University Hospital of Essen, Essen, Germany
[3]Department of Dermatology, University Hospital of Lübeck, Lübeck, Germany
[4]Department of Oncology-Pathology, Karolinska University Hospital, Stockholm, Sweden
[5]Department of Dermatology, University Hospital of Tübingen, Tübingen, Germany
[6]Department of Dermatology, University Medical Center Mainz, Mainz, Germany
[7]Department of Dermatology, University Hospital of Heidelberg, Heidelberg, Germany
[8]Deutsches Krebsforschungszentrum, Heidelberg, Germany
[9]Department of Dermatology, Ruhr University Bochum, Bochum, Germany
[10]Department of Dermatology, University Hospital Regensburg, Regensburg, Germany
[11]Department of Dermatology, Elbe Kliniken Buxtehude, Buxtehude, Germany
[12]Department of Dermatology, Saarland University Medical Center, Homburg, Germany
[13]Department of Dermatology-Oncology, University Hospital München, München, Germany
[14]Department of Dermatology, Skin Cancer Center Minden, Minden, Germany
[15]Department of Dermatology, Venereology and Allergology, University Medical Center Mannheim, Mannheim, Germany
[16]Deutsches Konsortium fur Translationale Krebsforschung, Essen, Germany
[17]Department of Pathology, University Hospital Essen, Essen, Germany
[18]Bioinformatics and Computational Biophysics, University of Duisburg-Essen, Duisburg, Germany

Acknowledgements We thank the patients who participated in this study, their families, and the staff members at the clinical centers who cared for them. We like to express our appreciation to Nalini Srinivas for critically proof reading the final version of the manuscript.

Contributors Conceptualisation: IS, SU, LK, H-US, DHa, DHo, and JCB; data curation: IS, SU, and JCB; formal analysis: IS, KH, and DHa; funding acquisition: JCB; investigation: IS, SU, LK, KH, DHa, DHo, and JCB; methodology: IS, SU, LK, DHa, DHo, and JCB; project administration: IS, SU, and JCB; resources: SU, LZ, PT, AM, HBA, LV, UL, TE, CL, JCH, TG, SH, PM, CP, LH, RG, JSU, DS, and JCB; software: IS, KH, and DHa; supervision: SU, and JCB; validation: IS, SU, KH, DHa, DHo, and JCB; visualisation: IS, SU, KH, DHa, DHo, and JCB; writing–original draft: IS, SU, and JCB; writing–review and editing: IS, SU, LK, PT, LV, TE, JCH, TG, RG, KH, DHa, DHo, H-US, DS, and JCB; IS, SU and JCB are guarantors of this study.

Funding This study was funded by the DKTK ED003

Competing interests SU declares research support from Bristol Myers Squibb and Merck Serono; speakers and advisory board honoraria from Bristol Myers Squibb, Merck Sharp & Dohme, Merck Serono, Novartis and Roche, and travel support from Bristol Myers Squibb, and Merck Sharp & Dohme. LZ served as consultant and/or has received honoraria from Roche, Bristol-Myers Squibb, Merck Sharp & Dohme, Novartis, Pierre-Fabre, and Sanofi; Research funding to institution: Novartis; travel support from Merck Sharp & Dohme, Bristol-Myers Squibb, Amgen, Pierre-Fabre, and Novartis, outside the submitted work. PT declares invited speaker's honoraria from Bristol-Myers Squibb, Novartis, MSD, Pierre-Fabre, CureVac, Roche, Kyowa Kirin, Biofrontera, advisory board honoraria from Bristol-Myers Squibb, Novartis, Pierre-Fabre, Merck Serono, Sanofi, Roche, Kyowa Kirin, and travel support from Bristol-Myers Squibb, and Pierre-Fabre. UL declares advisory board honoraria from MSD, Roche, Sanofi, Novartis, Sun Pharma, Almirall Hermal. TE declares consulting fees from BMS, Novartis, Roche, Pierre Fabre, Sanofi; board membership and payment for lectures in speakers bureau from Pierre Fabre, MSD, Roche, BMS, Novartis and Sanofi. CL reports advisory board honoraria from MSD, BMS, Roche, Pierre Fabre, Novartis, Sun Pharma, Sanofi, Kyowa Kirin, Almiral Hermal, Biontech, Merc; speakers fee from MSD, BMS, Roche, Pierre Fabre, Novartis, Sun Pharma, Sanofi, Merck; travel reimbusment from MSD, BMS, Roche, Pierre Fabre, Novartis, Sun Pharma, Sanofi, Kyowa Kirin, Almiral Hermal, Biontech and Merck. JCH declares research support from Bristol Myers Squibb; advisory board honoraria from Pierre Fabre, Sanofi, Sun Pharma and Merck Sharp & Dome; speakers honoraria from Bristol Myers Squibb, Merck Sharp & Dohme, Novartis, Roche, Sanofi and Almirall and travel support from Pierre Fabre. TG reports receiving speakers and/or advisory board honoraria from BMS, Sanofi-Grenzyme, MSD, Novartis Pharma, Roche, Abbvie, Almirall, Janssen Lilly, Pfizer, Pierre Fabre; speakers and/or advisory board honoraria from BMS, Sanofi-Grenzyme, MSD, Novartis, Pharma, Roche, Abbvie, Almirall, Janssen Lillly, Pfizer, Pierre Fabre. SH declares advisory boards honoraria from Pierre Fabre, MSD, BMS, Novartis, Sanofi. PM reports board membership and payment for lectures in speakers bureau from Pierre Fabre, GSK, MSD, Merck Germany, Roche, BMS, Novartis, Sanofi. P. Mohr reports research support (to institution): Bristol-MyersSquibb, Novartis, MSD. Honoraria for lectures (personally): Pierre Fabre, GSK, MSD, Merck Germany, Roche, BMS, Novartis, Sanofi, Amgen, SUN-Pharma, Roche Pharma, Bristol-MyersSquibb, Novartis, MSD, Almirall-Hermal, Amgen, Merck-Serono, Bayer, Pierre-Fabre, Sanofi. Honoraria for advisory boards: Pierre Fabre, GSK, MSD, Merck Germany, Roche, BMS, Novartis, Sanofi, Beiersdorf, Almiral-Hermal, AmgenBayersdorf, Roche Pharma, Bristol-MyersSquibb, Novartis, MSD, Almirall-Hermal, Amgen, Pierre-Fabre, Merck-Serono, SUN-Pharma, SUN, Merck-Serono, Sanofi. CP received honoraria (speaker honoraria or honoraria as a consultant) and travel support from Novartis, BMS, Roche, Merck Serono, MSD, Celgene, AbbVie, AMGEN, SUNPHARMA, Allergy Therapeutics and LEO. LMH served as consultant and/or has received honoraria from Amgen, BMS, Curevac, MSD, Novartis, Pierre-Fabre, Roche, Sanofi and Sun Pharma, outside the submitted work. Research funding to institution: Novartis. R. Gutzmer reports research support from Pfizer, Johnson & Johnson, Novartis, Amgen, MerckSerono, SUN Pharma; honoraria for lectures from Roche Pharma, Bristol-MyersSquibb, Novartis, MSD, Almirall-Hermal, Amgen, Merck-Serono, SUN, Pierre-Fabre, Sanofi, SUN Pharma, Bayer; honoraria for advice from Roche Pharma, Bristol-MyersSquibb, Novartis,

MSD, Almirall-Hermal, Amgen, Pierre-Fabre, Merck-Serono, 4SC, Incyte, SUN Pharma, Sanofi, Pfizer. JSU is on the advisory board or has received honoraria and travel support from Amgen, Bristol Myers Squibb, GSK, LeoPharma, Merck Sharp and Dohme, Novartis, Pierre Fabre, Roche, Sanofi outside the submitted work. H-US is an employee of Targos Molecular Pathology Inc. and reports research support from Novartis Oncology and received honoraria from MSD, BMS, Roche Pharma, Novartis Oncology, AstraZeneca, Eisai, Takeda, Molecular Health, outside of the submitted work. DS reports personal fees from Amgen, GSK, BMS, Novartis, Roche, Merck, Astra Zeneca, Merck-Serono, Pfizer, Incyte, Array Pierre Fabre, Sanofi Genzyme, Regeneron, 4Sc, InFlaRx, Neracare, Ultimovacs, SunPharma, Philogen, Immunocore, Sandoz-Hexal outside the submitted work. JCB is receiving speaker's bureau honoraria from Amgen, Pfizer, MerckSerono, Recordati and Sanofi; is a paid consultant/advisory board member/DSMB member for Almirall, Boehringer Ingelheim, InProTher, ICON, MerckSerono, Pfizer, 4SC, and Sanofi/Regeneron. His group receives research grants from Bristol-Myers Squibb, Merck Serono, HTG, IQVIA, and Alcedis.

Patient consent for publication Not applicable.

Ethics approval This study was approved by Ethics committee of the University Duisburg-Essen (11-4715; 17-7538-BO) Ethics board of Stockholm (Dnr 2010/1092-31/3).

Provenance and peer review Not commissioned; externally peer reviewed.

Data availability statement Data are available on reasonable request. All data relevant to the study are included in the article or uploaded as online supplemental information. All the raw data used within this manuscript are available on reasonable request to the corresponding author.

Supplemental material This content has been supplied by the author(s). It has not been vetted by BMJ Publishing Group Limited (BMJ) and may not have been peer-reviewed. Any opinions or recommendations discussed are solely those of the author(s) and are not endorsed by BMJ. BMJ disclaims all liability and responsibility arising from any reliance placed on the content. Where the content includes any translated material, BMJ does not warrant the accuracy and reliability of the translations (including but not limited to local regulations, clinical guidelines, terminology, drug names and drug dosages), and is not responsible for any error and/or omissions arising from translation and adaptation or otherwise.

ORCID iDs
Ivelina Spassova http://orcid.org/0000-0003-4663-7966
Selma Ugurel http://orcid.org/0000-0002-9384-6704
Patrick Terheyden http://orcid.org/0000-0002-5894-1677
Jürgen Christian Becker http://orcid.org/0000-0001-9183-653X

REFERENCES

1 Becker JC, Stang A, DeCaprio JA, *et al*. Merkel cell carcinoma. *Nat Rev Dis Primers* 2017;3:17077.
2 Nghiem PT, Bhatia S, Lipson EJ, *et al*. PD-1 blockade with pembrolizumab in advanced Merkel-cell carcinoma. *N Engl J Med* 2016;374:2542–52.
3 Topalian SL, Bhatia S, Amin A, *et al*. Neoadjuvant nivolumab for patients with resectable Merkel cell carcinoma in the CheckMate 358 trial. *J Clin Oncol* 2020;38:2476–87.
4 Kacew AJ, Dharaneeswaran H, Starrett GJ, *et al*. Predictors of immunotherapy benefit in Merkel cell carcinoma. *Oncotarget* 2020;11:4401–10.
5 Spassova I, Ugurel S, Terheyden P, *et al*. Predominance of central memory T cells with high T-cell receptor repertoire diversity is associated with response to PD-1/PD-L1 inhibition in Merkel cell carcinoma. *Clin Cancer Res* 2020;26:2257–67.
6 D'Angelo SP, Russell J, Lebbe C. Efficacy and safety of first-line avelumab treatment in patients with stage IV metastatic Merkel cell carcinoma: a preplanned interim analysis of a clinical trial. *JAMA Oncol* 2018;4:1–5.
7 Eisenhauer EA, Therasse P, Bogaerts J, *et al*. New response evaluation criteria in solid tumours: revised RECIST guideline (version 1.1). *Eur J Cancer* 2009;45:228–47.
8 Shen R, Postow MA, Adamow M, *et al*. LAG-3 expression on peripheral blood cells identifies patients with poorer outcomes after immune checkpoint blockade. *Sci Transl Med* 2021;13:eabf5107.
9 Bürkner P-C, Vuorre M. Ordinal regression models in psychology: a tutorial. *Adv Methods Pract Psychol Sci* 2019;2:77–101.
10 Thomas DC. Introduction: Bayesian models and Markov chain Monte Carlo methods. *Genet Epidemiol* 2001;21:S660–1.
11 Bürkner PC. Advanced Bayesian multilevel modeling with the R package brms. *R Journal* 2018;180:1–15.
12 Bürkner PC. brms: an R package for Bayesian multilevel models using Stan. *J Stat Softw* 2017;80:1–28.
13 Buuren Svan, Groothuis-Oudshoorn K. mice : Multivariate Imputation by Chained Equations in *R*. *J Stat Softw* 2011;45:1–67.
14 Collins GS, Reitsma JB, Altman DG, *et al*. Transparent reporting of a multivariable prediction model for individual prognosis or diagnosis (TRIPOD): the TRIPOD statement. *Ann Intern Med* 2015;162:55–63.
15 Henson SM, Riddell NE, Akbar AN. Properties of end-stage human T cells defined by CD45RA re-expression. *Curr Opin Immunol* 2012;24:476–81.
16 Walker JW, Lebbé C, Grignani G, *et al*. Efficacy and safety of avelumab treatment in patients with metastatic Merkel cell carcinoma: experience from a global expanded access program. *J Immunother Cancer* 2020;8:e000313.
17 Kugel CH, Douglass SM, Webster MR, *et al*. Age correlates with response to anti-PD1, reflecting age-related differences in intratumoral effector and regulatory T-cell populations. *Clin Cancer Res* 2018;24:5347–56.
18 Johnstone J, Parsons R, Botelho F, *et al*. T-Cell phenotypes predictive of frailty and mortality in elderly nursing home residents. *J Am Geriatr Soc* 2017;65:153–9.
19 De Maeyer RPH, Chambers ES. The impact of ageing on monocytes and macrophages. *Immunol Lett* 2021;230:1–10.
20 Knepper TC, Montesion M, Russell JS, *et al*. The genomic landscape of Merkel cell carcinoma and Clinicogenomic biomarkers of response to immune checkpoint inhibitor therapy. *Clin Cancer Res* 2019;25:5961–71.
21 Lanzavecchia A, Sallusto F. Regulation of T cell immunity by dendritic cells. *Cell* 2001;106:263–6.
22 Liu Q, Sun Z, Chen L. Memory T cells: strategies for optimizing tumor immunotherapy. *Protein Cell* 2020;11:549–64.
23 Sallusto F, Geginat J, Lanzavecchia A. Central memory and effector memory T cell subsets: function, generation, and maintenance. *Annu Rev Immunol* 2004;22:745–63.
24 Im SJ, Hashimoto M, Gerner MY, *et al*. Defining CD8+ T cells that provide the proliferative burst after PD-1 therapy. *Nature* 2016;537:417–21.
25 Kurtulus S, Madi A, Escobar G, *et al*. Checkpoint blockade immunotherapy induces dynamic changes in PD-1–CD8+ tumor-infiltrating T cells. *Immunity* 2019;50:181–94.
26 Miron M, Kumar BV, Meng W, *et al*. Human Lymph Nodes Maintain TCF-1 ^{hi} Memory T Cells with High Functional Potential and Clonal Diversity throughout Life. *J Immunol* 2018;201:2132–40.
27 Sade-Feldman M, Yizhak K, Bjorgaard SL, *et al*. Defining T cell states associated with response to checkpoint immunotherapy in melanoma. *Cell* 2018;175:998–1013.
28 Toews K, Grunewald L, Schwiebert S, *et al*. Central memory phenotype drives success of checkpoint inhibition in combination with CAR T cells. *Mol Carcinog* 2020;59:724–35.
29 Manjarrez-Orduño N, Menard LC, Kansal S, *et al*. Circulating T cell subpopulations correlate with immune responses at the tumor site and clinical response to PD1 inhibition in non-small cell lung cancer. *Front Immunol* 2018;9:1613.
30 Siddiqui I, Schaeuble K, Chennupati V, *et al*. Intratumoral Tcf1^{+}PD-1^{+}CD8^{+} T Cells with Stem-like Properties Promote Tumor Control in Response to Vaccination and Checkpoint Blockade Immunotherapy. *Immunity* 2019;50:195–211.
31 Mogilenko DA, Shpynov O, Andhey PS, *et al*. Comprehensive Profiling of an Aging Immune System Reveals Clonal GZMK^{+} CD8^{+} T Cells as Conserved Hallmark of Inflammaging. *Immunity* 2021;54:99–115.
32 Farah M, Reuben A, Spassova I, *et al*. T-Cell repertoire in combination with T-cell density predicts clinical outcomes in patients with Merkel cell carcinoma. *J Invest Dermatol* 2020;140:2146–56.

Supplementary Table S1. Detailed patient characteristics at baseline, during anti-PD-1/PD-L1 therapy, and follow-up.

Pat ID	Age (years) at baseline	Sex	ECOG at baseline	Immuno-suppression	Serum LDH at baseline	Serum CRP at baseline	neutro lympho ratio at baseline	Locali-sation of primary	M stage at therapy start	Organs involved	MCPyV status (tumor)	PD-L1 expression (tumor)	Previous chemo-therapy	Previous radio-therapy	Immune Checkpoint Inhibitors	Best Response	Trial of partici-pation	Year of treatment
1	86	M	0	No	normal	elevated	≥4	head + neck	M0	1	nd	nd	No	No	Avelumab	PD	No	2018
2	81	M	1	Yes (CLL; Prostate Cancer)	elevated	elevated	nd	extremities	M1a	2	positive	negative	No	No	Avelumab	PD	No	2018
3	79	F	1	No	normal	normal	<4	head + neck	M1c	1	positive	negative	Yes	Yes	Pembrolizumab	PD	No	2016
4	70	M	1	No	elevated	elevated	<4	extremities	M0	2	positive	nd	No	No	Avelumab	PD	No	2019
5	83	M	1	No	normal	normal	<4	head + neck	M1a	2	negative	positive	No	No	Avelumab	PD	No	2018
6	68	F	1	Yes (azathioprine, corticosteroids (rheumatoid arthritis, systemic lupus erythematodes, Hashimoto thyroiditis))	elevated	normal	≥4	extremities	M1c	2	positive	negative	No	Yes	Avelumab	PD	No	2017
7	66	M	0	No	normal	elevated	<4	trunk	M1a	1	nd	nd	No	No	Avelumab	PD	Yes	2017
8	62	M	0	No	elevated	normal	<4	unknown	M0	1	positive	positive	No	No	Avelumab	PD	Yes	2017
9	76	M	1	No	elevated	elevated	≥4	unknown	M1a	1	nd	nd	Yes	No	Avelumab	PD	Yes	2015
10	71	F	4	Yes (tacrolimus, corticosteroids (kidney transplantation))	elevated	elevated	<4	head + neck	M1c	2	negative	positive	No	No	Nivolumab	PD		2015
11	76	F	0	No	normal	nd	≥4	trunk	M1c	3	nd	nd	No	Yes	Pembrolizumab	PD	No	2017
12	75	M	1	Yes (CLL)	normal	nd	nd	unknown	M1b	2	positive	nd	No	No	Pembrolizumab	PD	No	2018
13	77	F	1	No	elevated	nd	nd	unknown	M1b	2	nd	nd	No	No	Pembrolizumab	PD	Yes	2019
14	86	M	0	No	elevated	nd	nd	unknown	M1c	3	nd	nd	No	No	Pembrolizumab	PD	Yes	2019
15	67	F	1	No	elevated	elevated	≥4	head + neck	M1a	1	positive	positive	No	Yes	Pembrolizumab	PD	No	2016
16	66	F	1	No	elevated	elevated	<4	unknown	M0	2	nd	nd	Yes	Yes	Pembrolizumab	PD	No	2016
17	72	M	1	No	elevated	elevated	<4	extremities	M1a	1	positive	negative	Yes	Yes	Pembrolizumab	PD	No	2016
18	62	M	0	No	elevated	elevated	≥4	extremities	M1c	2	nd	nd	No	Yes	Avelumab	PD	Yes	2016
19	79	M	0	No	elevated	elevated	<4	trunk	M1c	3	nd	nd	No	No	Avelumab	PD	No	2018
20	68	M	1	Yes (azathioprine (myasthenia gravis)	elevated	elevated	nd	head + neck	M0	1	positive	negative	No	Yes	Nivolumab	PD	No	2017
21	64	M	0	Yes (NH-Lymphom)	normal	nd	<4	extremities	M1c	4	nd	nd	No	Yes	Avelumab	PD	No	2018
22	77	M	0	Yes (CLL)	elevated	normal	<4	extremities	M1a	1	nd	nd	No	No	Avelumab	PD	No	2019

23	83	M	1	No	elevated	elevated	≥4	extremities	M0	1	nd	nd	Yes	No	Avelumab	PD	Yes	2015
24	75	M	2	No	normal	elevated	≥4	extremities	M1c	2	negative	nd	No	Yes	Avelumab	PD	No	2018
25	56	M	1	No	normal	nd	<4	extremities	M1a	2	nd	nd	No	Yes	Pembrolizumab	PD	No	2016
26	74	M	0	No	elevated	elevated	≥4	extremities	M1c	5	nd	nd	Yes	Yes	Avelumab	PD	Yes	2015
27	75	F	1	No	elevated	normal	≥4	unknown	M1a	1	positive	negative	Yes	No	Pembrolizumab	PD	No	2016
28	82	F	1	No	elevated	normal	<4	extremities	M1a	2	nd	positive	No	Yes	Avelumab	PD	No	2018
29	83	M	3	No	elevated	elevated	≥4	unknown	M1c	2	nd	nd	No	Yes	Avelumab	PD	No	2019
30	59	M	0	Yes (CLL)	normal	normal	<4	extremities	M1a	2	positive	positive	No	No	Nivolumab	PD	No	2017
31	66	F	2	No	elevated	elevated	<4	trunk	M1a	1	nd	nd	No	No	Avelumab	PD	Yes	2017
32	56	F	0	No	elevated	normal	<4	extremities	M1c	3	nd	nd	No	Yes	Avelumab	PD	Yes	2016
33	78	F	0	No	nd	nd	nd	trunk	M1c	3	nd	nd	Yes	Yes	Avelumab	PD	No	2017
34	37	M	0	No	normal	elevated	<4	trunk	M1b	2	nd	positive	Yes	Yes	Avelumab	PD	Yes	2015
35	85	M	1	No	elevated	elevated	<4	extremities	M1c	4	positive	positive	No	No	Pembrolizumab	PD	No	2017
36	66	M	1	Yes (CLL)	elevated	elevated	nd	trunk	M1a	1	negative	positive	No	No	Pembrolizumab	PD	No	2018
37	53	M	1	Yes (MTX in clippers syndrome and steroids)	elevated	elevated	≥4	extremities	M1c	3	nd	nd	No	Yes	Avelumab	PD	No	2018
38	80	M	0	No	elevated	elevated	≥4	unknown	M1c	2	nd	nd	No	Yes	Avelumab	PD	Yes	2017
39	80	M	0	Yes (rheumatoid arthritis (until 11/2016 MTX + Ankinra, prednisolone 5mg daily))	elevated	elevated	≥4	head + neck	M1c	5	nd	nd	Yes	Yes	Pembrolizumab	PD		2016
40	69	M	0	Yes (CML, osteomyelofibrosis)	elevated	elevated	≥4	extremities	M1c	2	nd	nd	No	No	Avelumab	PD		2017
41	68	M	0	Yes (CLL)	elevated	elevated	nd	unknown	M1a	1	nd	nd	Yes	No	Pembrolizumab	SD	No	2017
42	77	M	1	Yes (CLL, melanoma)	normal	elevated	≥4	head + neck	M1c	1	negative	positive	Yes	Yes	Pembrolizumab	SD	No	2016
43	75	M	0	No	elevated	elevated	<4	extremities	M0	1	nd	nd	Yes	No	Avelumab	SD	No	2018
44	78	M	1	No	elevated	elevated	<4	extremities	M1c	3	nd	negative	Yes	No	Avelumab	SD	Yes	2015
45	48	F	0	No	normal	normal	<4	unknown	M1a	1	positive	positive	Yes	Yes	Pembrolizumab	SD	No	2017
46	76	M	0	No	normal	normal	<4	head + neck	M1c	3	negative	positive	No	No	Avelumab	SD	No	2018
47	72	F	0	No	elevated	elevated	≥4	head + neck	M1a	1	positive	negative	Yes	Yes	Nivolumab	SD	Yes	2015
48	60	F	0	No	normal	nd	<4	extremities	M1c	4	nd	nd	No	No	Avelumab	SD	No	2019
49	83	M	1	No	elevated	elevated	<4	unknown	M1c	4	nd	nd	Yes	Yes	Pembrolizumab	SD	No	2014
50	82	M	0	No	normal	elevated	<4	head + neck	M0	1	nd	nd	Yes	No	Avelumab	SD	Yes	2016

51	63	M	0	No	elevated	nd	<4	extremities	M1c	4	nd	nd	No	Yes	Avelumab	SD	No	2018
52	90	F	2	No	elevated	elevated	nd	head + neck	M0	1	nd	nd	No	No	Avelumab	SD	No	2017
53	80	F	0	Yes (non-Hodgkin lymphoma (cyclophosphamide, doxorubicine, vincristine, prednisone); anal carcinoma)	normal	normal	<4	head + neck	M1c	2	negative	negative	No	No	Nivolumab	SD	No	2017
54	78	M	0	Yes (CLL, melanoma)	elevated	normal	<4	extremities	M1c	2	positive	nd	No	Yes	Pembrolizumab	SD	No	2017
55	79	M	0	No	elevated	elevated	≥4	extremities	M1c	3	nd	nd	No	Yes	Pembrolizumab	SD		2017
56	83	F	1	Yes (multiple myeloma, polycythemia vera)	elevated	elevated	<4	extremities	M1c	2	nd	nd	No	Yes	Avelumab	SD		2017
57	73	M	1	No	elevated	elevated	≥4	trunk	M1c	4	negative	positive	Yes	Yes	Avelumab	SD	Yes	2016
58	68	M	0	No	normal	nd	<4	unknown	M1a	1	nd	nd	No	No	Avelumab	SD	No	2018
59	70	M	0	No	elevated	elevated	<4	extremities	M1a	1	positive	positive	Yes	Yes	Pembrolizumab	SD	No	2016
60	69	F	2	No	normal	normal	<4	head + neck	M1c	2	nd	nd	No	No	Avelumab	SD	No	2018
61	82	M	1	No	normal	nd	<4	head + neck	M1c	3	nd	nd	No	No	Avelumab	PR	No	2017
62	86	M	nd	No	normal	normal	<4	extremities	M0	1	nd	nd	No	No	Avelumab	PR	No	2018
63	71	M	0	No	elevated	normal	<4	extremities	M1a	2	positive	positive	No	Yes	Pembrolizumab	PR	No	2017
64	89	M	0	Yes (non-small cell lung cancer; prostate cancer)	normal	normal	<4	trunk	M1c	3	positive	negative	No	Yes	Pembrolizumab	PR	No	2017
65	65	M	0	No	normal	nd	<4	extremities	M1a	1	positive	negative	No	Yes	Nivolumab	PR	Yes	2016
66	73	M	0	No	normal	normal	≥4	extremities	M1a	1	nd	nd	No	Yes	Nivolumab	PR	No	2015
67	90	M	1	No	elevated	elevated	≥4	head + neck	M1c	2	nd	nd	No	Yes	Pembrolizumab	PR		2017
68	74	M	1	No	elevated	elevated	≥4	extremities	M1c	2	positive	negative	Yes	Yes	Pembrolizumab	PR	No	2015
69	57	F	0	No	normal	normal	<4	extremities	M1a	1	nd	nd	No	No	Avelumab	PR	No	2018
70	68	M	0	No	normal	normal	≥4	head + neck	M1c	3	negative	negative	Yes	No	Avelumab	PR	Yes	2015
71	59	M	0	no	normal	nd	nd	unknown	M1b	3	nd	nd	Yes	Yes	Pembrolizumab	PR	No	2017
72	55	M	0	No	elevated	elevated	≥4	unknown	M1c	2	nd	nd	No	Yes	Pembrolizumab	PR	No	2016
73	85	M	0	No	elevated	nd	<4	trunk	M1c	1	nd	nd	No	Yes	Pembrolizumab	PR	No	2016
74	76	M	0	No	elevated	elevated	<4	extremities	M1c	2	nd	positive	Yes	No	Pembrolizumab	PR	No	2015
75	86	M	1	No	elevated	elevated	≥4	trunk	M1c	2	positive	positive	No	No	Pembrolizumab	PR		2017

76	84	M	1	No	elevated	normal	≥4	trunk	M1c	4	positive	positive	No	Yes	Avelumab	PR	No	2018
77	61	M	0	No	elevated	normal	<4	head + neck	M1c	3	nd	nd	No	Yes	Avelumab	PR	Yes	2016
78	76	M	0	No	normal	elevated	<4	unknown	M1a	1	nd	nd	No	Yes	Pembrolizumab	PR		2017
79	48	M	1	Yes (promyelocytic leukemia)	elevated	elevated	<4	trunk	M0	1	positive	negative	No	Yes	Avelumab	PR	No	2018
80	85	M	1	No	elevated	nd	nd	unknown	M1c	3	positive	nd	No	Yes	Pembrolizumab	PR	Yes	2019
81	50	M	1	No	elevated	elevated	≥4	extremities	M0	1	positive	positive	Yes	No	Nivolumab	PR	No	2016
82	71	F	1	No	normal	nd	nd	unknown	M1a	1	nd	nd	No	No	Pembrolizumab	PR	Yes	2019
83	52	M	0	No	elevated	elevated	≥4	trunk	M1a	1	nd	nd	No	Yes	Avelumab	PR	No	2018
84	82	M	1	Yes (renal cell carcinoma, urothelial carcinoma)	elevated	elevated	<4	extremities	M1a	1	nd	negative	No	Yes	Avelumab	PR		2018
85	76	M	1	Yes (CLL)	nd	nd	nd	unknown	M1a	1	nd	nd	Yes	No	Nivolumab	PR	No	2016
86	82	F	2	No	elevated	nd	nd	unknown	M1c	3	nd	nd	No	No	Pembrolizumab	PR	No	2017
87	82	M	0	No	elevated	nd	nd	unknown	M1c	2	positive	nd	No	No	Pembrolizumab	PR	No	2019
88	77	M	0	No	normal	elevated	≥4	head + neck	M1c	1	nd	nd	No	Yes	Pembrolizumab	PR		2016
89	75	F	1	No	elevated	elevated	≥4	extremities	M1b	1	nd	nd	No	No	Avelumab	PR		2018
90	87	M	1	No	elevated	elevated	<4	extremities	M0	1	nd	nd	No	No	Avelumab	PR	No	2017
91	65	M	0	No	normal	normal	<4	head + neck	M1c	1	nd	nd	No	No	Avelumab	CR	Yes	2017
92	59	M	1	No	normal	normal	<4	unknown	M1c	2	nd	positive	Yes	Yes	Pembrolizumab	CR	No	2016
93	96	M	1	No	normal	nd	≥4	trunk	M0	1	nd	nd	No	No	Avelumab	CR	No	2018
94	64	M	0	No	normal	elevated	<4	trunk	M1c	1	nd	nd	No	Yes	Pembrolizumab	CR	No	2016
95	61	F	0	Yes (azathioprine (myasthenia gravis))	elevated	elevated	<4	trunk	M1c	1	nd	nd	No	Yes	Pembrolizumab	CR	No	2016
96	69	M	1	No	elevated	normal	<4	extremities	M1a	2	positive	negative	Yes	Yes	Avelumab	CR	Yes	2016
97	79	M	0	No	elevated	normal	≥4	extremities	M1a	1	nd	nd	No	Yes	Nivolumab	CR	Yes	2016
98	57	F	0	No	normal	nd	≥4	unknown	M1c	3	positive	negative	No	Yes	Nivolumab	CR	Yes	2015
99	76	M	0	No	elevated	elevated	<4	extremities	M1a	1	negative	nd	No	No	Pembrolizumab	CR	No	2017
100	72	F	0	No	normal	elevated	≥4	extremities	M1a	1	nd	positive	Yes	Yes	Avelumab	CR	No	2017
101	71	M	0	No	normal	normal	<4	extremities	M0	2	nd	nd	No	Yes	Avelumab	CR	No	2018
102	79	F	0	No	elevated	normal	<4	trunk	M1a	2	positive	nd	No	Yes	Avelumab	CR	Yes	2016
103	83	F	1	No	elevated	elevated	≥4	unknown	M1a	2	nd	nd	No	No	Pembrolizumab	CR		2017
104	80	M	0	No	normal	normal	<4	head + neck	M1c	1	nd	nd	No	Yes	Avelumab	CR		2017

105	60	M	0	No	elevated	elevated	nd	extremities	M1c	5	nd	nd	Yes	Yes	Pembrolizumab	CR	No	2016
106	82	F	0	No	nd	nd	nd	extremities	M1c	2	nd	nd	No	No	Avelumab	CR	No	2018
107	62	M	0	No	normal	nd	nd	extremities	M1c	1	nd	nd	No	No	Pembrolizumab	CR	No	2016
108	75	F	1	No	normal	nd	nd	head + neck	M1c	2	nd	nd	Yes	No	Pembrolizumab	CR	No	2017
109	83	F	0	No	normal	nd	nd	head + neck	M0	1	nd	nd	No	No	Avelumab	CR	No	2018
110	83	M	0	No	normal	normal	nd	head + neck	M0	1	nd	nd	No	No	Avelumab	CR	No	2018
111	79	M	0	No	nd	nd	nd	trunk	M1a	1	nd	nd	No	Yes	Avelumab	CR	No	2017
112	77	M	0	No	elevated	nd	nd	unknown	M1c	2	positive	nd	No	No	Nivolumab	CR	No	2016
113	77	F	0	No	elevated	nd	nd	unknown	M1a	1	positive	nd	No	No	Pembrolizumab	CR	No	2017
114	64	M	0	No	normal	nd	nd	unknown	M1a	1	positive	nd	No	No	Nivolumab	CR	No	2017

Characteristics of total patient cohort (n=118). Best response is related to the anti-PD-1/PD-L1 therapy. Patients are sorted according to their change in sum of longest diameters of target lesions from baseline to best response (see **Figure 1**). Abbreviations: M – male; F – female; CLL – chronic lymphocytic leukemia; CML – chronic myelogenous leukemia; CR – complete response, PR – partial response; SD – stable disease; PD – progressive disease; nd – no data available.

Supplementary Table S2. Antibodies and procedures used for multiplex immunohistochemical staining

Position	Antibody	Clone/Company	Dilution	Incubation	AG[1] retrieval	TSA[3] dye
Panel 1						
1	CD4	PerkinElmer	1:50	30 min	AR[2] 9	520
2	CD8	PerkinElmer	1:100	30 min	AR 9	570
3	CD20	PerkinElmer	1:200	30 min	AR 6	540
4	FoxP3	PerkinElmer	1:400	30 min	AR 6	620
5	CD68	PerkinElmer	1:1000	30 min	AR 6	650
6	SYN	SP11/Abcam	1:1000	Over night	AR 6	690
Panel 2						
1	CD27	EPR8569/Abcam	1:2000	30 min	AR 9	520
2	GZMB	ab4059/Abcam	1:100	30 min	AR 6	570
3	TCF7	C63D9/Cell Signaling	1:100	30 min	ÂR 6	540
4	CD45RA	4KB5/Santa Cruz	1:500	30 min	AR 6	620
5	CD45R0	UCHL1/Novus Bio.	1:1000	30 min	AR 9	650
6	SYN	SP11/Abcam	1:1000	Over night	AR 6	690

[1]AG: antigen; [2]AR: antigen retrieval buffer with pH 6 (AR6) and pH 9 (AR9); SYN: synaptophysin; [3]TSA: Tyramide Signal Amplification

Supplementary Table S3. Markers for detection/quantification of immune cell types in MCC tissue.

Cell type	**Used markers for detection/quantification**
Leukocytes	CD45RA(+) or CD45RO(+)
Regulatory T cells	CD4(+)FoxP3(+)
Central memory T cells	CD27(+)TCF1(+)CD45RO(+)
Effector T cells	GZMB(+)CD45RA(+)
Monocytes/macrophages	CD68(+)
B cells	CD20(+)

Supplementary Table S4. Mean percentage of positively stained cells to total cell number per analysed area for each analyzed MCC samples. For quantification analysis three randomly chosen tissue regions at the juxta-tumoral area as well as in the intra-tumoral area were processed in a semi-automatic fashion by InForm Tissue Analysis software.

Response to ICI	total cell number (in three tissue regions)		% to total cell number for all three fields											
			Ø CD4(+)		ØFoxP3(+)		Ø CD4(+)FoxP3(+)		Ø CD8(+)		Ø CD20(+)		Ø CD68(+)	
	Juxta-tumoral	Intra-tumoral	Juxta-tumoral	Intra-tumoral	Juxta-tumoral	Intra-tumoral	Juxta-tumoral	Intra-tumoral	Juxta-tumoral	Intra-tumoral	Juxta-tumoral	Intra-tumoral	Juxta-tumoral	Intra-tumoral
PR	7034	6042	1,94	0,83	1,98	0,69	1,97	0,68	7,97	4,63	5,40	2,60	3,20	1,99
CR	7019	6710	0,94	14,22	6,26	3,91	3,27	2,13	30,20	20,57	16,77	13,01	2,05	1,54
SD	5845	6390	0,63	0,90	1,76	1,32	0,03	0,03	10,50	12,79	4,41	4,14	2,94	3,91
PR	5443	5167	1,52	1,38	1,60	1,23	0,49	0,55	12,46	10,52	2,76	2,11	4,14	4,47
PR	5160	7304	3,60	0,09	2,75	0,26	1,47	0,19	3,58	0,23	2,01	0,03	3,51	0,64
SD	6414	8940	0,16	0,02	1,76	1,32	0,43	0,00	2,58	0,20	1,27	0,18	1,89	0,29
CR	3196	4847	1,02	1,05	2,61	3,38	0,83	0,83	3,30	7,27	0,21	0,40	1,55	3,60
PR	4703	7812	5,37	0,00	0,00	0,00	0,00	0,00	31,20	7,33	0,00	0,00	3,73	0,30
PR	3604	4782	0,50	2,25	0,00	0,00	0,00	0,00	11,92	9,04	0,40	1,00	1,75	1,00
CR	4434	5039	0,25	0,30	0,00	0,00	0,00	0,00	14,21	2,65	0,00	0,00	3,50	0,45
PR	3005	2707	9,30	3,90	0,90	1,10	0,90	1,10	42,62	15,88	4,65	0,22	4,98	3,56
PD	-	5114	-	0,00	-	0,15	-	0,00	-	0,96	-	0,00	-	0,60
PD	4366	5065	0,11	0,00	0,13	0,00	0,08	0,00	0,00	0,07	0,00	0,00	0,28	0,39
PD	4302	4052	1,46	0,33	2,53	1,79	0,81	0,23	3,30	0,63	0,20	0,08	2,27	1,57
PD	3184	4720	2,86	2,66	3,35	2,30	2,80	2,02	6,63	3,12	6,04	2,06	1,76	1,12
PD	7849	6980	1,32	1,91	0,49	0,24	0,27	0,14	6,23	7,90	7,47	4,32	1,18	2,10
PD	2644	6392	11,20	3,45	0,00	0,00	0,00	0,00	8,00	7,88	0,10	1,05	18,30	9,10
PD	3518	3648	2,00	0,10	0,00	0,00	0,00	0,00	9,04	6,15	0,00	0,00	1,73	0,35
PD	4531	5983	0,15	0,05	0,00	0,00	0,00	0,00	19,50	6,50	6,25	0,00	7,95	0,40
PD	4227	5709	0,40	0,00	0,00	0,00	0,00	0,00	2,59	0,96	0,00	0,00	5,50	0,20
PD	3218	3146	0,20	0,55	0,00	0,00	0,00	0,00	8,00	1,05	0,10	0,10	4,45	0,75

Supplementary Table S5. Mean percentage of positively stained cells to total cell number per analysed area for each analyzed MCC samples. For quantification analysis of three randomly chosen tissue regions at the juxta-tumoral area as well as in the intra-tumoral area were processed in a semi-automatic fashion by InForm Tissue Analysis software.

Response to ICI	total cell number (in three tissue regions)		% to total cell number for all three fields													
			Ø CD45RO(+)		Ø CD45RA(+)		Ø CD27(+)		Ø TCF7(+)		Ø CD27(+)TCF7(+) CD45RO(+)		Ø GZMB(+)		Ø GZMB(+)CD 45RA(+)	
	Juxta-tumoral	Intra-tumoral	Juxta-tumoral	Intra-tumoral	Juxta-tumoral	Intra-tumoral	Juxta-tumoral	Intra-tumoral	Juxta-tumoral	Intra-tumoral	Juxta-tumoral	Intra-tumoral	Juxta-tumoral	Intra-tumoral	Juxta-tumoral	Intra-tumoral
PR	7182	6571	26,33	9,19	3,20	1,94	13,63	11,41	7,30	2,62	1,39	0,24	0,17	0,07	0,00	0,00
CR	6943	7694	15,92	10,72	5,83	2,14	5,54	4,68	3,97	2,33	0,65	0,35	4,19	3,77	0,99	0,64
SD	6992	6464	0,06	34,64	25,87	19,80	11,97	41,78	5,57	23,73	0,00	11,98	0,30	3,40	0,10	1,73
PR	5727	7196	46,29	68,40	48,63	62,30	19,53	17,59	66,97	64,60	17,09	15,29	6,40	4,39	3,50	2,63
PR	5665	6431	30,33	29,15	3,25	4,46	48,10	17,83	8,07	8,45	2,25	2,69	2,58	1,53	0,11	0,08
SD	4908	6575	22,27	0,87	7,30	0,60	12,76	0,60	15,73	0,30	3,84	0,39	0,43	0,23	0,23	0,17
CR	6234	6641	1,05	3,20	0,79	1,06	2,43	4,23	1,93	2,87	0,42	1,41	1,43	5,21	0,30	0,76
PR	3370	3178	0,03	0,43	0,00	0,00	0,00	0,33	0,00	0,27	0,00	0,00	0,67	7,66	0,00	0,00
PR	7442	7688	10,30	40,73	14,50	37,70	0,07	3,00	0,00	0,03	0,00	8,63	2,40	0,63	0,10	0,20
CR	4622	5001	25,33	34,20	11,03	7,39	4,70	3,57	14,57	18,61	4,73	4,87	2,53	4,15	1,01	1,52
PR	6429	5660	17,33	5,98	17,83	1,58	8,45	1,07	23,96	2,33	11,61	2,77	0,77	1,77	0,52	0,22
PD	-	3758	-	0,00	-	0,00	-	0,00	-	0,00		0,00	-	0,00	-	0,00
PD	4379	4131	0,90	0,70	0,10	0,60	0,17	0,23	0,03	0,03	0,00	0,00	0,20	0,80	0,05	0,60
PD	5559	5342	8,60	1,05	11,63	1,27	0,87	1,60	0,00	0,00	0,00	0,00	2,10	0,17	2,03	0,17
PD	3324	4748	4,39	0,98	2,80	2,60	15,40	9,39	7,07	6,49	0,86	0,54	1,53	0,73	0,37	0,30
PD	7149	6999	25,12	13,47	28,47	21,93	17,97	7,35	5,80	2,65	11,79	4,60	0,27	0,13	0,03	0,07
PD	4178	4513	5,20	7,23	2,37	1,10	1,80	1,17	10,33	3,87	1,29	0,83	0,45	0,13	0,12	0,07
PD	6552	8078	0,00	0,17	0,00	0,00	0,00	0,00	0,00	0,00	0,00	0,00	0,00	0,00	0,00	0,00
PD	6834	6977	31,99	3,09	3,69	1,03	32,37	3,22	8,69	0,28	1,32	0,02	24,42	3,70	2,26	0,46
PD	6422	6715	5,97	0,67	0,30	0,26	3,22	1,48	5,33	0,42	0,13	0,02	3,08	1,48	0,14	0,08
PD	4835	4637	2,30	0,87	0,99	0,55	0,47	0,48	0,42	0,51	0,00	0,00	1,80	1,33	0,51	0,43

Supplementary Table S6: Clinical variable values comparing patients with PD-1 blockade to those with PD-L1 blockade.

	All patients *N*=114 (100%)	**PD-1 inhibitor therapy n=57 (100%)**	**PD-L1 inhibitor therapy n=57 (100%)**
Patient characteristics			
Sex			
male	82 (72%)	40 (70%)	42 (74%)
female	32 (28%)	17 (30%)	15 (26%)
Age			
< 70	40 (35%)	19 (33%)	21 (37%)
≥ 70	74 (65%)	38 (67%)	36 (63%)
Overall performance status (ECOG)			
0	64 (56%)	32 (56%)	32 (56%)
≥1	49 (43%)	25 (44%)	24 (42%)
Immunosuppression			
no	92 (81%)	44 (77%)	48 (84%)
yes	22 (19%)	13 (23%)	9 (16%)
LDH			
normal	43 (38%)	21 (37%)	22 (39%)
elevated	67 (59%)	35 (61%)	32 (56%)
CRP			
normal	30 (26%)	11 (19%)	19 (33%)
elevated	55 (48%)	27 (47%)	28 (49%)
NLR			
< 4	54 (47%)	22 (39%)	32 (56%)
≥ 4	35 (31%)	17 (30%)	18 (32%)
Tumor characteristics			
Localization of primary			
head and neck	24 (21%)	11 (19%)	13 (23%)
extremities	44 (39%)	17 (30%)	27 (47%)
trunk	19 (17%)	7 (12%)	12 (21%)
unknown	15 (13%)	10 (18%)	5 (9%)
Metastatic stage (AJCC)			
M0	17 (15%)	3 (5%)	14 (25%)
M1a	36 (32%)	21 (37%)	15 (26%)
M1b/M1c	61 (53%)	33 (58%)	28 (49%)
Organs onvolved			
1	51 (45%)	26 (46%)	25 (44%)
> 1	63 (55%)	31 (54%)	32 (56%)
MCPyV status (tumor)			
negative	10 (9%)	5 (9%)	5 (9%)
positive	32 (28%)	24 (42%)	8 (14%)
n.d.	72 (63%)	28(49%)	44 (77%)
PD-L1 (tumor)			
negative	17 (15%)	10 (17%)	7 (12%)
positive	21 (18%)	13 (23%)	8 (14%)
n.d.	76 (67%)	34 (60%)	42 (74%)
Therapeutic interventions			
Previous radiotherapy			
no	55 (48%)	24 (42%)	31 (54%)
yes	59 (52%)	33 (58%)	26 (46%)
Previous chemotherapy			
no	83 (73%)	38 (67%)	45 (79%)
yes	31 (27%)	19 (33%)	12 (21%)
Therapy response			
CR	24 (21%)	13 (23%)	11 (19%)
PR	30 (26%)	19 (33%)	11 (19%)
SD	20 (18%)	9 (16%)	11 (19%)
PD	40 (35%)	16 (28%)	24 (43%)

Abbreviations: AJCC, American Joint Committee on Cancer; ECOG, Eastern Cooperative Oncology Group; LDH, lactate dehydrogenase; MCPyV, Merkel cell polyomavirus; NLR, neutrophil to lymphocyte ratio.

Supplementary Figure 1

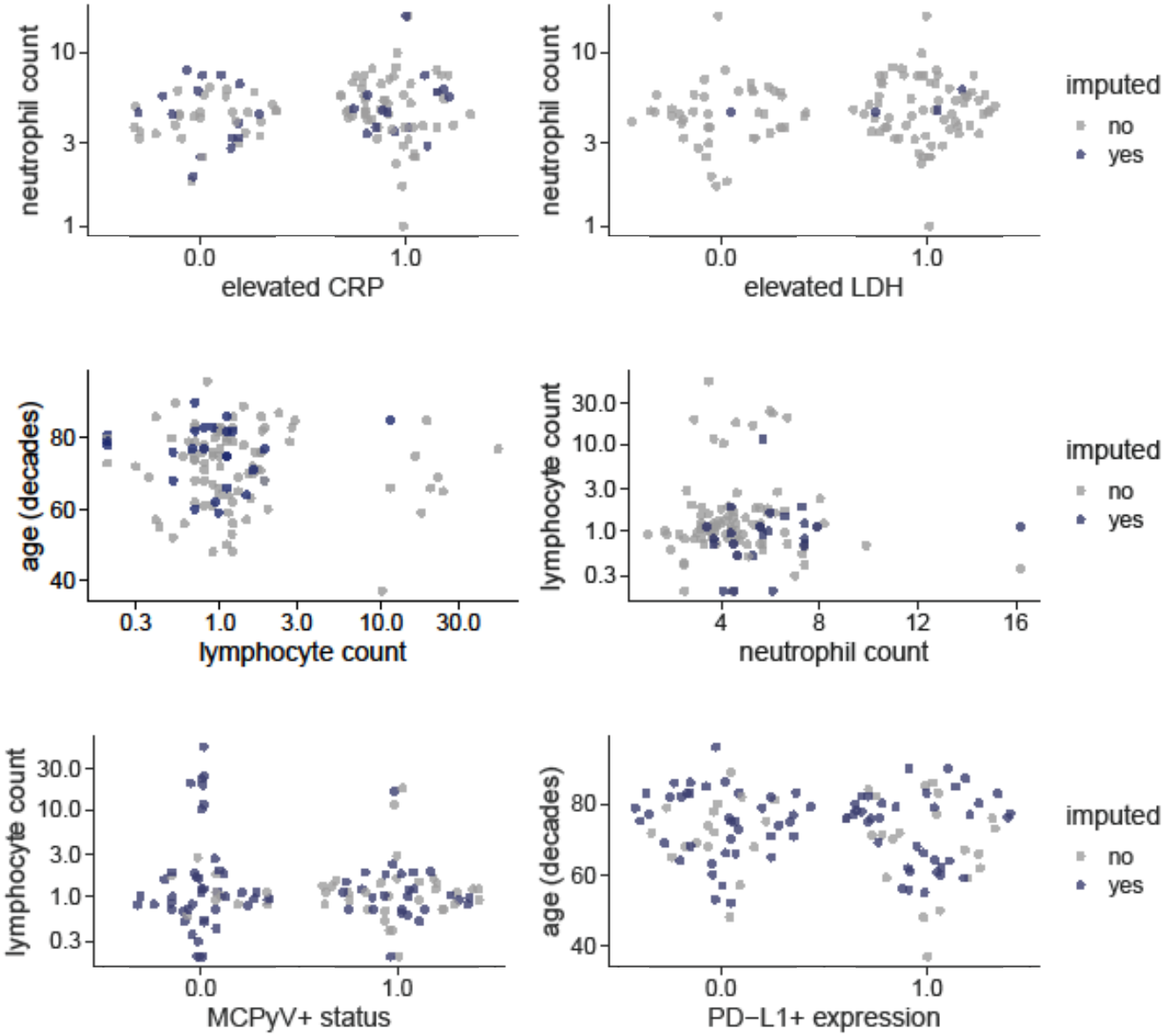

Scatter plots comparing the actually observed data with 30 imputed data sets of clinical parameters with missing values in the Bayesian ordinal regression model. CRP – C-reactive protein; LDH – Lactate dehydrogenase; MCPyV – Merkel cell polyomavirus.

Supplementary Figure 2

LOO sequential model with proportional odds assumption (fit_1):

```
          Estimate   SE
elpd_loo   -192.0 10.5
p_loo        50.9  7.5
looic       384.1 20.9

Pareto k diagnostic values:
                         Count Pct.    Min. n_eff
(-Inf, 0.5]   (good)     99    86.8%   8414
 (0.5, 0.7]   (ok)       12    10.5%   1834
   (0.7, 1]   (bad)       2     1.8%   830
   (1, Inf)   (very bad)  1     0.9%   36
```

LOO sequential model without proportional odds assumption, category-specific parameters for all predictors (fit_2):

```
          Estimate   SE
elpd_loo   -207.8 11.0
p_loo        79.0  7.2
looic       415.6 22.0

Pareto k diagnostic values:
                         Count Pct.    Min. n_eff
(-Inf, 0.5]   (good)     89    78.1%   9770
 (0.5, 0.7]   (ok)       23    20.2%   751
   (0.7, 1]   (bad)       1     0.9%   633
   (1, Inf)   (very bad)  1     0.9%   20
```

LOO sequential model with proportional odds assumption, category-specific parameters for most relevant predictors (immunosuppression, organs_greater_1) (fit_3):

```
          Estimate   SE
elpd_loo   -190.4 11.3
p_loo        49.3  8.2
looic       380.8 22.6

Pareto k diagnostic values:
                         Count Pct.    Min. n_eff
(-Inf, 0.5]   (good)     100   87.7%   10642
 (0.5, 0.7]   (ok)        11    9.6%   1806
   (0.7, 1]   (bad)        2    1.8%   271
   (1, Inf)   (very bad)   1    0.9%   8
```

LOO comparisons (fit 1 vs. fit 2 vs. fit 3):

```
      elpd_diff se_diff
fit     0.0       0.0
fit_3  -1.7       1.6
fit_2 -17.4       6.0
```

Leave-one-out cross-validation (LOO) demonstrates that the choosen model has a similar ELPD (expected log-predictive density, a measure of its ability to generalize to unseen data) as a sequential model without category-specific effects, meaning that including category-specific effects does not improve model performance and the proportional odds assumption does not have a strong effect on the model conclusions.

Supplementary Figure 3

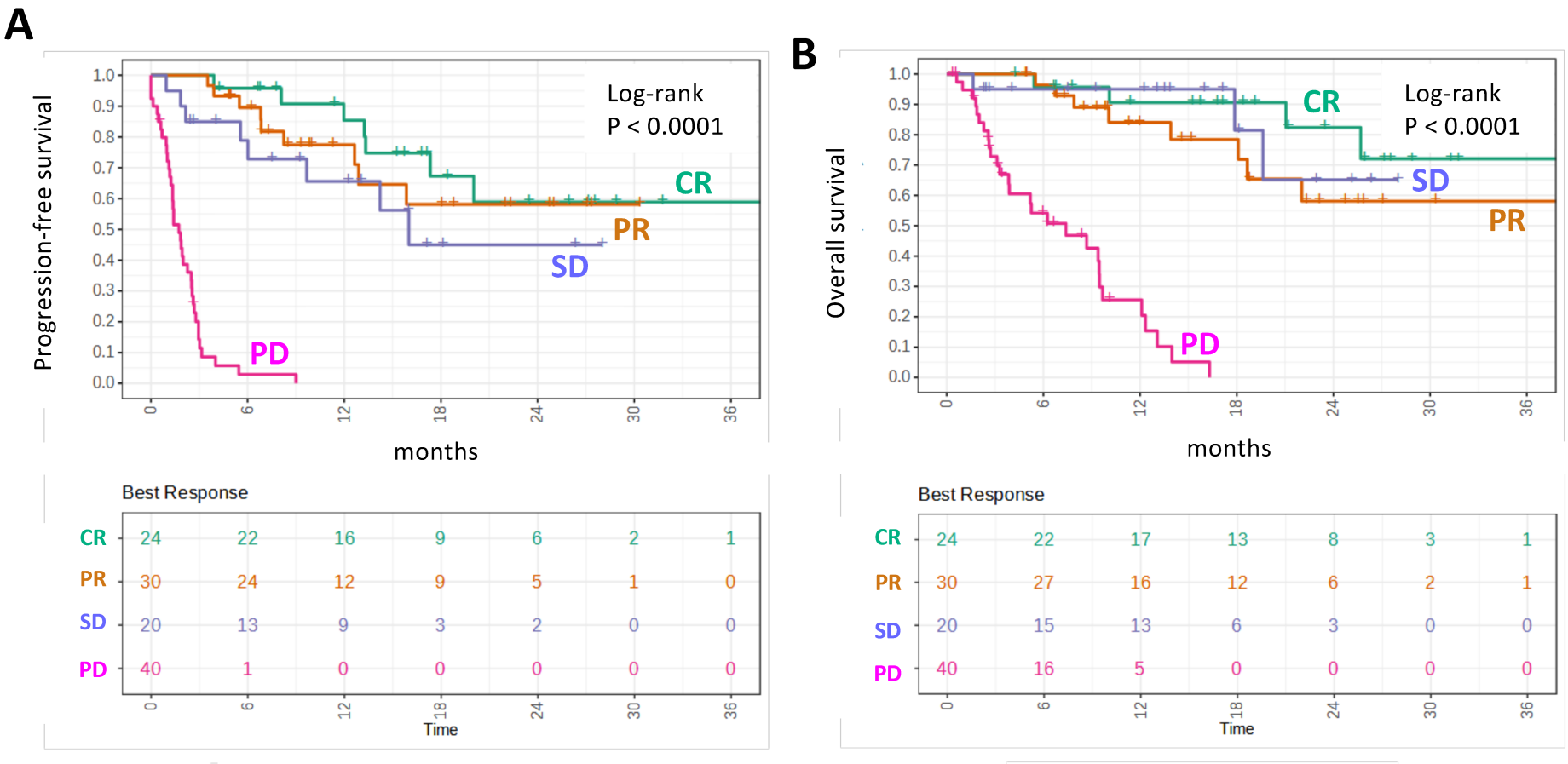

Survival characteristics of n = 114 advanced MM patients upon ICI therapy. (A, B) Kaplan Meier plots depicting (A) progression free (PFS) and (B) overall survival (OS) by BOR (CR, green, n=24; PR, orange, n = 30; SD, purple, n=20; PD, magenta, n=40) after therapy start. Patients after 36 months are all censored. CR, complete response; PR, partial response; SD, stable disease; PD, progressive disease.

Supplementary Figure 4

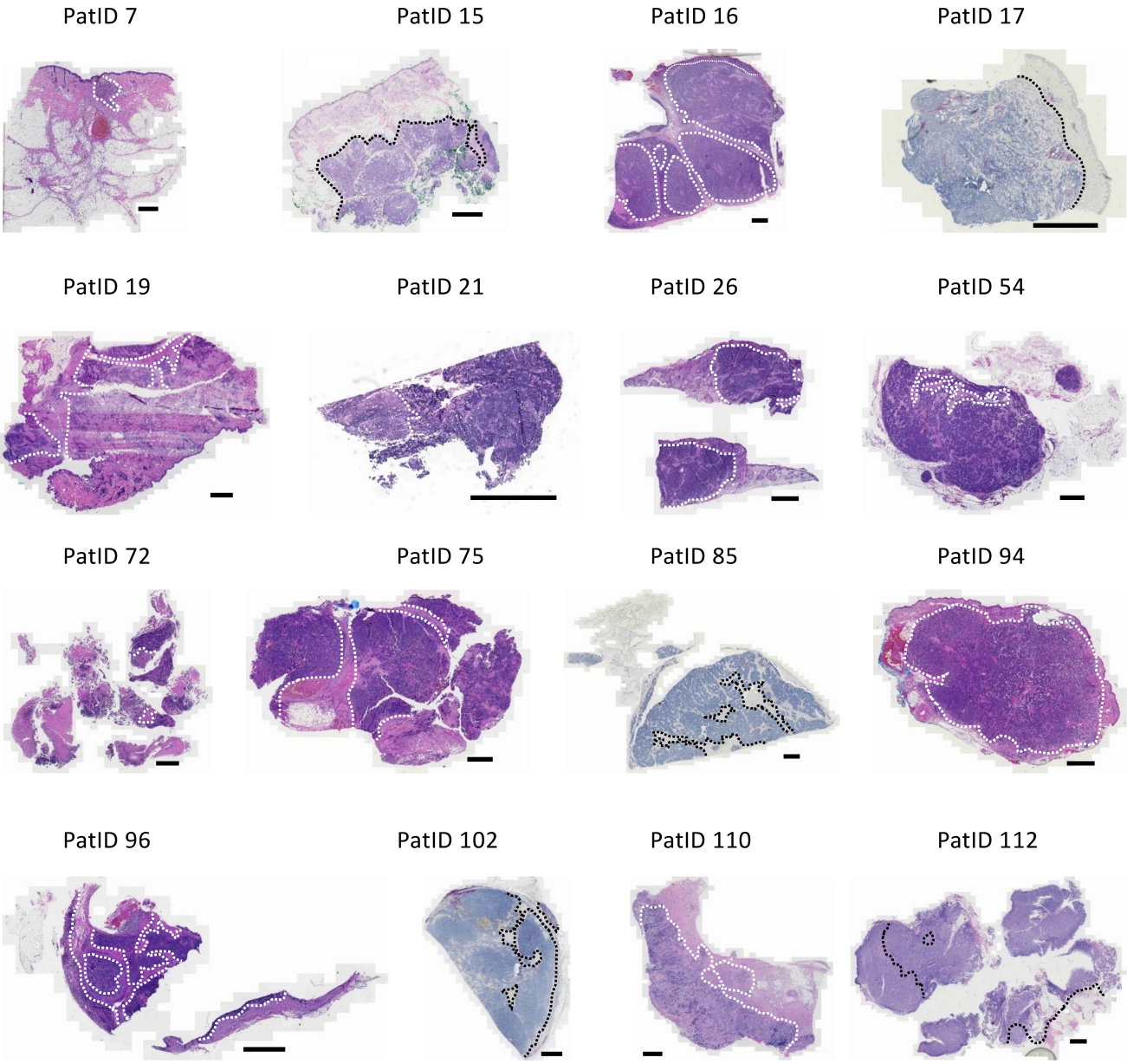

Whole slide scans of H&E stained tissue samples used for mIF based analysis of the immune infiltrate. Dotted lines (black/white) indicate separation between juxtra-tumoral and intra-tumoral areas (scale bar 2mm). Out of 114 samples, 21were subjected to mIF analysis. From these, 16 samples were already H&E stained for diagnostic reasons and were used here to depict the intra- and juxtra-tumoral regions. Slides were scanned with the Zeiss AxioScanZ.1 with 10x magnification.

Supplementary Figure 5

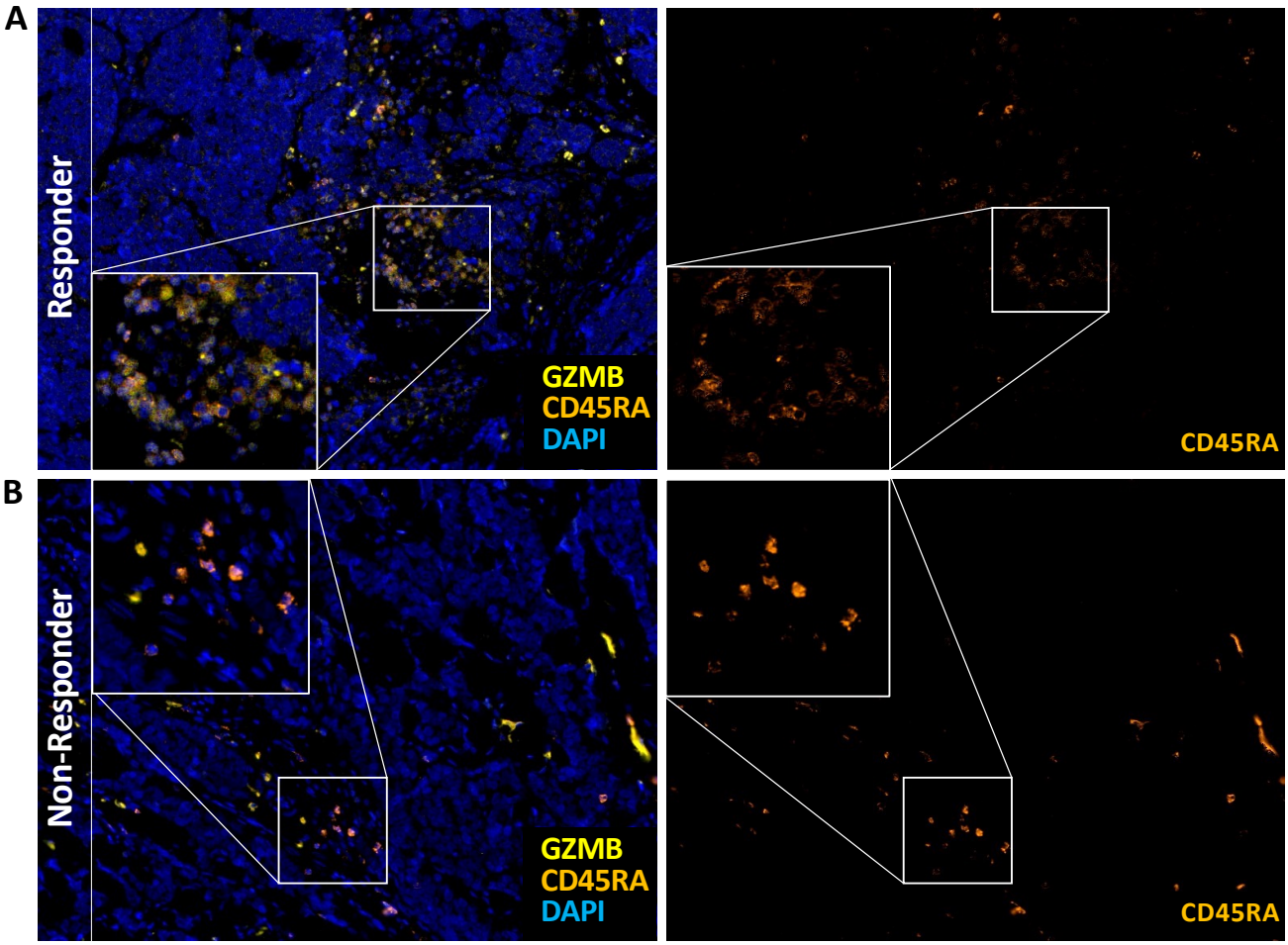

Excerpt of the multiplexed immunofluorescence staining of pre-treatment tumor tissue from a representative patient with disease control (A) and disease progression (B). Left: Co-expression of CD45RA (orange) and GZMB (yellow) displays high abundance of effector T cells in disease control. Right: Overall elevated presence of CD45RA positive cells in therapy responding patients.(20x magnification, DAPI counterstain)

Applying a cumulative ordinal regression model to infer possible biomarkers associated with response to PD-1/PD-L1 inhibition in Merkel cell carcinoma

Summary
Merkel cell carcinoma a is type of neuroendocrine skin cancer that in some cases can be treated with anti-PD-1/PD-L1 antibodies that act as immune checkpoint inhibitors and therefore enhance immune response against tumor cells. In an effort to identify biomarkers that distinguish treatment responders from non-responders, data of 114 patients had been collected and analyzed using a cumulative ordinal regression model. Conditioned on the model and the observed data, there is moderate statistical evidence that absence of immunosuppression, usage of anti-PD-1 antibodies (as opposed to anti-PD-L1 antibodies), and limited spread of the main tumor are associated with a higher probability of responding to the treatment.

Contents

1. Dataset

The dataset had been collected from 4 patients with Merkel cell carcinoma. All patients were either treated with anti-PD-1 or anti-PD-L1 antibodies and treatment response was classified into progressive disease (PD), stable disease (SD), partial response (PR) and complete response (CR). In total, there are 19 different predictors:

- gender (categorical: male, female)
- primary localisation (categorical: head + neck, occult, extremities, trunk)
- immunosuppression (binary)
- tumor PD-L1 expression (binary)
- MCPyV+ status (binary)
- prior chemotherapy (binary)
- prior radiotherapy (binary)
- checkpoint inhibition (categorical: PD-1, PD-L1)
- metastasic stage (categorical: M0, M1a, M1b/M1c)
- ≥ 2 organs involved (binary)
- elevated LDH levels (binary)
- elevated CRP levels (binary)
- neutrophil count at therapy start (numeric)
- lymphocyte count at therapy start (numeric)
- neutrophil/lymphocyte ratio (NLR) ≥ 4 (binary)
- ECOG performance status ≥ 1 (binary)
- age ≥ 70 years (binary)
- year of therapy start (ordered categorical)
- participation in a clinical trial (binary)

2. Introduction

To analyze these data, we fit a Bayesian model. This has several advantages:

A unique feature of Bayesian statistics is that it allows to describe model parameters with probability distributions. This means that instead of point estimates (with more or less reliable standard deviations) we obtain

a distribution of parameter values that is consistent with the observed data. In this way, it is possible to quantify the uncertainty of the estimates.

Additionally, Bayesian statistics provides an accessible way to test models: By comparing data generated under the model's assumptions to the actually observed data, it is possible to identify important aspects of the dataset that the model fails to capture, and subsequently improve the model until it is consistent with the observed data.

The dataset also contains missing values, and Bayesian statistics allows to incorporate data points where some of the inputs are missing in such a way that the uncertainty of the missing values directly translates into uncertainty of the estimates.

3. Model description

The treatment response (progressive disease, stable disease, partial response or complete response) is on an ordinal scale, which means that the different levels have an inherent order, e.g a partial response is clearly better than stable disease.

Unfortunately, statistical models that are applied to this kind of data often do not adequately account for this order: In practice, a common approach is to encode the categories as increasing integer values (1, 2, 3, …) and to apply a linear regression model. While this preserves the order, it assumes equal distances between the outcomes, which means that the distance between progressive- and stable disease is identical to the distance between partial response and complete response. Other common approaches involve multinomial models (which ignore the order) or fitting logistic regression models after arbitrarily binarizing the response.

All these approaches share the common problem that they do not make efficient use of the available data and might lead to over- or underestimated effect sizes [1]. For instance when binning the data into two categories (responder and non-responder), patients with a partial response have the same influence on the overall estimates as patients with a complete response. The grouping is often also arbitrary, for example in terms of survival time, our data shows that patients with stable disease are actually more similar to partial- and complete responders than to patients with progressive disease (data not shown).

3.1 Cumulative ordinal regression model

To circumvent the aforementioned issues, we apply a cumulative ordinal regression model, which adequately takes the order between the categories into account.

The main idea of the cumulative regression model is to regard the tendency of a patient to respond to the treatment as a latent (= unobserved) variable that is determined by the patient characteristics. By convention, this latent variable is usually assumed to be distributed according to a logistic distribution with a scale of 1 and a mean that is determined by the predictor values for that patient.

The logistic distribution with a scale of 1 closely resembles a normal distribution with a standard deviation of 1.6. In fact, the exact choice of distribution does not matter in practice and other choices are possible, e.g. using a standard normal distribution instead would lead to a class of models called probit models (whereas the cumulative regression model using the logistic distribution is a generalization of the logistic regression model for ordered responses with more than two categories).

The probabilities of the four possible response categories are then determined by three thresholds that are also estimated.

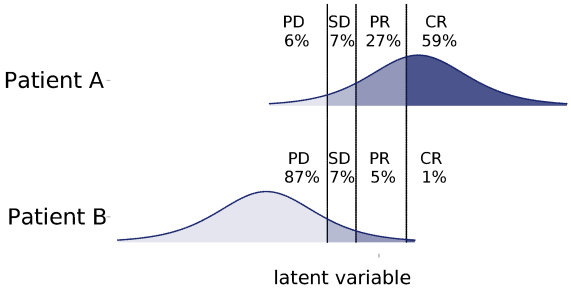

Figure 1. Distributions of the inferred latent variable for two patients in the dataset. PD: progressive disease, SD: stable disease, PR: partial response, CR: complete response.

Figure 1 shows the distribution of the latent variable for two patients in the dataset along with the 3 estimated thresholds (vertical lines). Patient A has predictor values that favor treatment response, whereas Patient B has predictor values that do not favor treatment response. The probability for each of the response categories is given by the area under the curve that is enclosed by the corresponding thresholds. Please note that, as we fit the model in a Bayesian fashion, neither the location of

the latent variables nor the tresholds are fixed values (as shown in Fig. 1), but follow some distribution of values that are consistent with the observed data.

In formula notation, the model can be written as:

$$\begin{aligned}
\mu_i &= \beta_{\text{age}} \cdot x_{\text{i, age}} + \beta_{\text{LDH}} \cdot x_{\text{i, LDH}} \dots \\
p(\text{PD})_i &= \int_{-\infty}^{\tau_1} \text{logistic_distribution}(\mu_i, 1) dx \\
p(\text{SD})_i &= \int_{\tau_1}^{\tau_2} \text{logistic_distribution}(\mu_i, 1) dx \\
p(\text{PR})_i &= \int_{\tau_2}^{\tau_3} \text{logistic_distribution}(\mu_i, 1) dx \\
p(\text{CR})_i &= \int_{\tau_3}^{\infty} \text{logistic_distribution}(\mu_i, 1) dx
\end{aligned} \tag{1}$$

,

where

- μ_i is the location of the latent variable for patient i,
- β_{age} is the β coefficient for the predictor age,
- $x_{\text{i, age}}$ is the indicator variable of patient i for age (in this case, 0 if patient i's age is $\geq$ 70 years, 1 otherwise),
- $p(\text{PD})_i$ is the probability of a progressive disease response
- τ_1, τ_2, τ_3 are the three estimated tresholds.

The β coefficients of the predictors are of main interest in this analysis, as they give information on whether or not a predictor is associated with a higher probability of responding to the treatment. A more comprehensive explanation of ordinal regression models that is also accessible without a background in statistics is given in [2].

3.2 Model fitting

Fitting the model to the dataset was done with the R software package 'brms' [3], which utilizes 'Stan' [4] in the background. Student t priors with 7 degrees of freedom and a standard deviation of 1 were chosen as weakly informative priors for the β coefficients. This is in line with the Stan prior choice recommendations [1]. The t distribution has a similar shape as the normal distribution, but with higher density in the tail areas. In this way, we rule out unreasonably large parameter values (e.g. anything larger than 10-15 for coefficients on the log-odds scale), but the model is still flexible enough to allow for values that might make sense. Model fit is performed numerically by Markov chain Monte Carlo. In total, 2000 samples from 4 different Markov chains were generated. We use the split-$\hat{R}$ diagnostic [5, 6] to identify possible Markov chain convergence issues. All parameters satisfied $\hat{R} < 1.01$, the effective sample size N_{eff} [7] exceeded 1000 in all cases.

[1] https://github.com/stan-dev/stan/wiki/Prior-Choice-Recommendations

4. Model results

Figure 2 shows marginal posterior distributions of the estimated β coefficients. Values larger than 0 denote that these predictors favor a response to the treatment, whereas values less than 0 favor treatment non-response. The width of the distribution gives an impression of the uncertainty of the estimate: A distribution tightly concentrated around some value means that the dataset allows for a precise estimate of that parameter, while a broader distribution means that the data is consistent with a wide range of parameter values.

Please note that all these estimates are conditioned on the model and the observed data, which means that they are not a statement about the general population of patients with Merkel cell carcinoma.

Most of estimates include 0, which means that the absence of association between that predictor and the treatment response is a reasonable explanation for the observed data. The widths of the distributions are also broad, so while no effect is a possible explanation, it could also be quite large.

Notable exceptions are the predictors immunosuppression and organs involved, where most of the probability mass is located at values less than 0 (denoting they are associated with a decreased probability of treatment response); and the use of an anti-PD-1 antibody, where most of the probability mass is located at values greater than 0 (denoting it is associated with an increased probability of treatment response), as compared to checkpoint inhibition with an anti-PD-L1 antibody.

4.1 Average Predictive Comparisons

As with logistic regression models, the β coefficients of cumulative ordinal regression models are in units of log-odds, which means that a value of 1 of the corresponding predictor increases the expected log-odds of the next higher response category by 1.

This has the disadvantage that it is difficult to have an intuition about the effect size, i.e. whether an increase in the log-odds by 1 corresponds to a large, moderate or small change. To circumvent this issue, we show average predictive comparisons in addition to the regression coefficients.

Briefly, average predictive comparisons are calculated as the expected change in the response associated with a unit difference in one of the inputs. A technical description of average predictive comparisons is given in [8]. In this analysis, it allows us to reinterpret the regression coefficients (which are in units of log-odds) into a summary that is on the probability scale.

Figure 2 shows average predictive comparisons for each of the model inputs. They were calculated with respect to having at least a partial response to the treatment, e.g. for immunosuppression, values between -0% and -40% denote that comparing a patient with immunosuppression to an otherwise identical patient without immunosuppression, the patient with immunosuppression has (on average) a 0% to 40% lower probability of having at least a partial response to treatment.

As a result of the limited sample size, the uncertainty around the estimates is rather large. It also shows that just because a predictor includes 0%, it should not be confused with having no association with the treatment response, because the data is still consistent with large effect sizes in either direction.

5. Imputing missing values

The dataset contains missing values in some of the predictors. Standard practice is usually to delete them, either by row-wise exclusion (removing all samples that contain any missing value), or by removing the predictors that contain missing values.

With only 114 patients, removing all samples that contain missing values would mean to remove import information.

As a more sensible approach, multiple imputation with the R package mice [9] was used instead. In multiple imputation, several imputed versions of the dataset are created where the missing values are replaced with plausible values. The imputed datasets are identical for the non-missing entries, but differ in the imputed values. The uncertainty about the missing values is reflected in the degree of variation between the datasets.

To translate these different datasets into as single estimate, we simply fit the model independently on each dataset and combine the posterior samples of each model fit. In this way, the uncertainty of the missing values propagates directly into uncertainty of the estimates.

6. Model testing

A useful way to test Bayesian models is called posterior predictive check. In posterior predictive checks, the inferred parameter estimates are used to sample an arbitrary number of new datasets that are generated under the model's assumptions. By comparing these datasets to the actually observed dataset, it is possible to identify aspects of the data that the model fails to capture.

One possible way to perform a posterior predictive check for the model described here is to compare the observed proportion of the different treatment response categories to the proportion of treatment response categories expected under the model's assumptions. Figure 3 shows a histogram of the proportion of patients with progressive disease, stable disease, partial response and complete response in the generated datasets with the actually observed proportions highlighted in blue. The observed proportions lie directly in the center of what is expected by the model.

Another form of posterior predictive check focuses on individual predictions instead. For each patient, the expected probability that a given patient has at least a partial response to the antibody treatment is calculated. If the model produces reasonable estimates, we expect that patients with a higher estimated probability really do respond more frequently to the treatment than patients with a lower estimated probability.

Figure 4 shows a so-called calibration plot. All 114 patients were sorted according to their expected probability of having at least a partial response to the treatment and placed into 7 distinct bins. For each bin, the mean probability of having a partial response is plotted against the observed proportion of patients in that bin which at least partially respond to the treatment. As each uncertainty interval around the observed proportion touches the diagonal line, this type of posterior predictive check shows again no large discrepancies between expected and observed data.

In conclusion, the posterior predictive checks show that the clinical data is consistent with data expected under the model's assumptions.

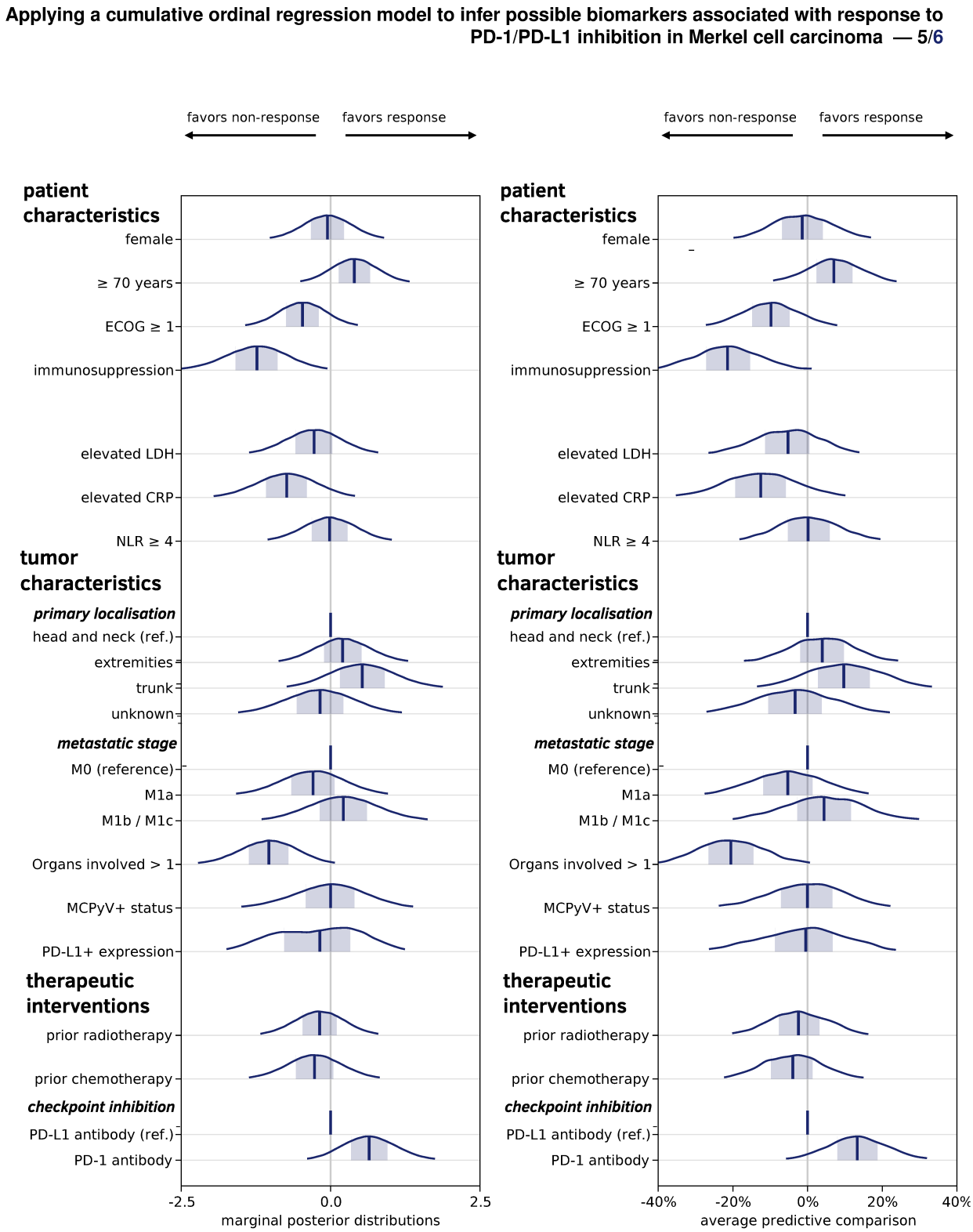

Figure 2. Marginal posterior distributions of β coefficients (left) and average predictive comparisons of the expected probability of having at least a partial response to the treatment (right). The regression coefficients of the full model have been projected onto a probability scale.

Applying a cumulative ordinal regression model to infer possible biomarkers associated with response to PD-1/PD-L1 inhibition in Merkel cell carcinoma — 6/6

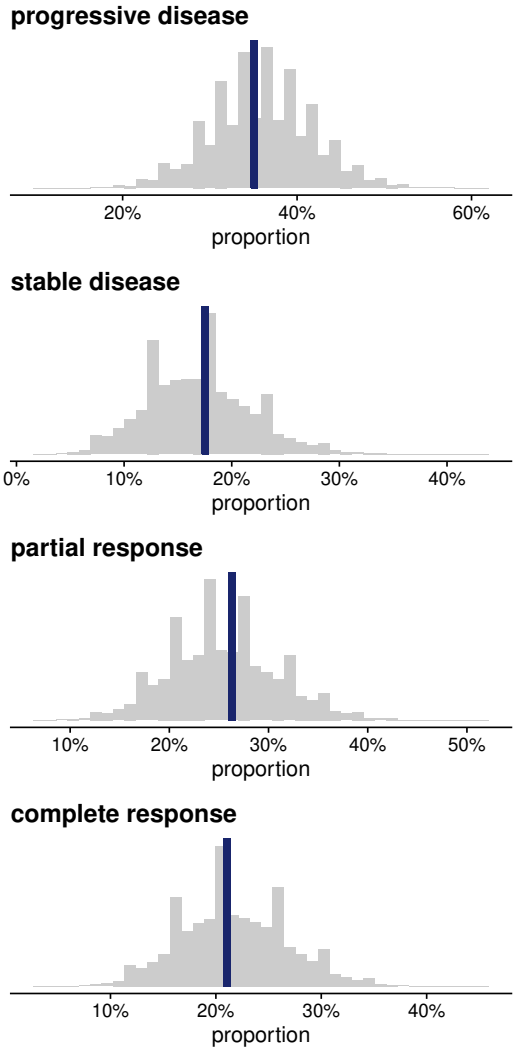

Figure 3. Expected proportion of each response category under the model (histogram) vs. observed proportion (blue line).

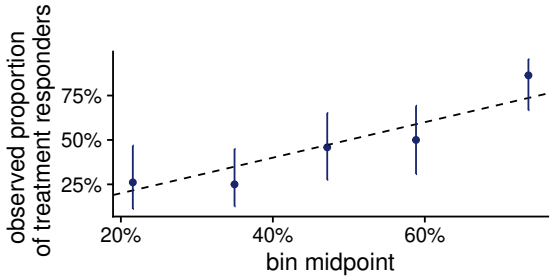

Figure 4. Calibration plot of proportion of patients with at least a partial response to the treatment.

References

[1] Torrin M. Liddell and John K. Kruschke. Analyzing ordinal data: Support for a Bayesian approach. *SSRN Electronic Journal*, 2015.

[2] Paul-Christian Bürkner and Matti Vuorre. Ordinal regression models in psychology: A tutorial. 2:77–101, 2019.

[3] Paul-Christian Bürkner. brms: An R package for Bayesian multilevel models using Stan. *Journal of Statistical Software*, 80(1), 2017.

[4] Bob Carpenter, Andrew Gelman, Matthew D. Hoffman, Daniel Lee, Ben Goodrich, Michael Betancourt, Marcus Brubaker, Jiqiang Guo, Peter Li, and Allen Riddell. Stan: A probabilistic programming language. *Journal of Statistical Software*, 76(1), 2017.

[5] Andrew Gelman and Donald B. Rubin. Inference from iterative simulation using multiple sequences. *Statistical Science*, 7(4):457–472, nov 1992.

[6] Andrew Gelman, John B Carlin, Hal S Stern, David B Dunson, Aki Vehtari, and Donald B Rubin. *Bayesian data analysis*. CRC press, 2013.

[7] Stan Development Team. *Stan Modeling Language Users Guide and Reference Manual, 2.23. https://mc-stan.org*, 2021.

[8] Andrew Gelman and Iain Pardoe. 2. Average Predictive Comparisons for models with nonlinearity, interactions, and variance components. *Sociological Methodology*, 37(1):23–51, aug 2007.

[9] Stef van Buuren and Karin Groothuis-Oudshoorn. mice: Multivariate imputation by chained equations in R. *Journal of Statistical Software*, 45(3), 2011.